Chem Soc Rev

Photochemistry and Photophysics of MOFs: Steps Towards MOF-based Sensing Enhancements

Journal:	*Chemical Society Reviews*
Manuscript ID	CS-REV-12-2017-000861.R1
Article Type:	Review Article
Date Submitted by the Author:	15-Feb-2018
Complete List of Authors:	Dolgopolova, Ekaterina; University of South Carolina, Department of Chemistry and Biochemistry Rice, Allison; University of South Carolina, Department of Chemistry and Biochemistry Martin, Corey; University of South Carolina, Department of Chemistry and Biochemistry Shustova, Natalia; University of South Carolina, Department of Chemistry and Biochemistry

Journal Name

ARTICLE

Photochemistry and Photophysics of MOFs: Steps Towards MOF-based Sensing Enhancements

Received 00th January 20xx,
Accepted 00th January 20xx

DOI: 10.1039/x0xx00000x

www.rsc.org/

Ekaterina A. Dolgopolova,† Allison M. Rice,† Corey R. Martin, and Natalia B. Shustova*

In this review, we highlight how recent advances achieved in the fields of photochemistry and photophysics of metal-organic frameworks (MOFs) could be applied towards the engineering of next generation MOF-based sensing devices. In addition to high surface area and structural tunability, which are crucial for efficient sensor development, progress in the field of MOF-based sensors could rely on the combination of MOF light-harvesting ability, understanding energy transfer processes within a framework, and application of MOF-based photocatalysis towards sensing enhancement. All photophysical concepts could be integrated within one material to improve efficiency and selectivity of sensing devices. Thus, the focus of this review is shifted towards a "beyond the pores" approach, which could foreshadow new guidelines for sensor engineering.

MOFs as Advanced Sensors

For the next generation of MOF-based sensing devices, it could be pivotal to shift from the typically applied "classical" pore-exclusion topological paradigm[1–15] to utilization of advances in the areas of MOF photophysics and photochemistry.[16–28] In this review, we will refashion light harvesting, energy transfer (ET), and photocatalytic processes, which could occur within a porous crystalline framework towards the enhancement of MOF-based sensing. There have already been a number of experimental studies highlighting advantages of some facets in the discussed strategy. For instance, ET, in combination with the high surface area of MOFs, has already been applied towards sensing of acetone,[29,30] melamine,[31] explosives,[32] metal cations (e.g., Hg^{2+}),[33] benzene,[34] anions (e.g., F^-),[34,35] or formaldehyde.[35] Another intriguing class of MOF-sensors coupled to ligand-to-metal and/or metal-to-metal ET is lanthanide-based frameworks (Ln-MOFs), which have been applied as noninvasive thermometers working in a wide temperature range.[36–43]

An inspiration for understanding and utilization of the mentioned photophysical processes could be taken from the natural photosystem, where the efficiency relies on the cooperative effect of several hundred chromophores (Fig. 1). MOFs could also be used as a tool for such chromophore

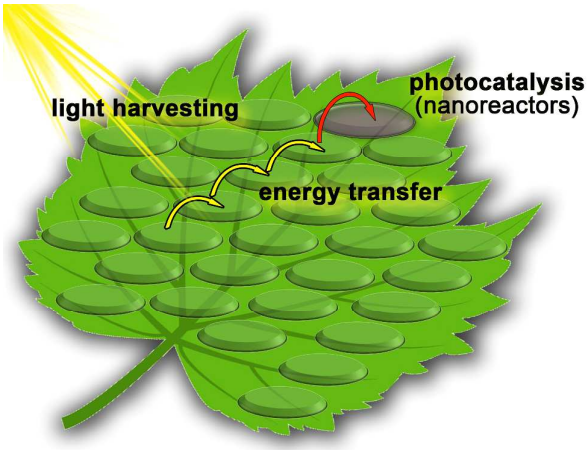

Fig. 1 A schematic representation of processes occurring in the natural photosystem, which could be utilized for the enhanced efficiency of next generation MOF-based sensing devices.

arrangement through utilization of the self-assembly approach.[44–60] The coordination of organic linkers to metal nodes allows for the organization of chromophores in a well-defined manner, preventing exciton quenching or shortened exciton lifetimes.[61] The high degree of chromophore organization achieved in a MOF structure also provides a basis for systematic structure-function studies, focused on the ability of photon capture with the subsequent exciton migration to a reaction center.[61] In contrast to amorphous polymers, the distances and angles between chromophores in MOFs can be determined by single-crystal X-ray diffraction and tuned through ligand design or variation of synthetic conditions. The latter aspect is crucial for the understanding and modeling of short- and long-range ET processes in such

Department of Chemistry and Biochemistry, University of South Carolina, 631 Sumter Street, Columbia, SC 29208, USA.
E-mail: shustova@sc.edu
† Denotes equal contribution.

complex systems, which is essential for the rational design of MOF-based sensors coupled to ET. [2,62–64] Finally, MOFs can be used as a "three-in-one" sensing platform, which integrates the three aspects of artificial photosynthesis: photon absorption, generation of charge-separated excited states, and charge transfer to a reaction center into a single material to enhance sensing efficiency.[62,65–68]

In parallel with photon capture occurring in the natural photosystem, the first step for the preparation of MOF-based sensors coupled to ET is light harvesting.[2,61,62,66,69–73] In addition to a high degree of chromophore ordering, MOF structural diversity allows for the integration of light-harvesting units as either framework building blocks or guests. For instance, coupling of two light-harvesting cores can be efficiently achieved in MOFs, as well as the integration of quantum dots (QDs) possessing large absorption cross sections.[74] As the next step after light harvesting, MOFs can also be engineered to provide directional ET by including different framework functionalities. For instance, ligand-to-ligand, metal-to-metal, metal-to-ligand (or ligand-to-metal), and guest-to-MOF ET pathways could occur in a MOF matrix, among which some have already been successfully applied for sensing.[36,41,75]

Just as in the case of the natural photosystem, where a series of redox reactions take place at a reaction center, MOFs can be utilized as efficient photocatalysts, and newly formed products could be the analytes of interest for subsequent chemosensing.[62,65,67,76–81] A MOF consists of well-defined homogeneously distributed metal sites, which could be catalytically active and tuned towards specific catalytic transformations and subsequent sensing of a wide range of products. Such spatial separation of the metal sites (in contrast to metal nanoparticle sintering), in combination with the high surface area of MOFs, distinguishes these materials for use in the realm of photocatalysis, as well as sensing. Furthermore, MOF cavities could be utilized as tunable nanoreactors, which can also result in simultaneous product formation and *in situ* detection.

To summarize, this review will foreshadow a new spin on the application of the "triple nature" of MOFs as light-harvesting materials, as platforms to achieve directional ET, and as efficient photocatalysts towards development of novel sensing principles in MOFs.

Light Harvesting as a First Step for Sensor Development

Light harvesting is a first step for rational development of an ET-coupled sensor. MOFs have emerged as a promising artificial light-harvesting system due to their highly ordered structures which can contain chlorophyll analogues to absorb light for subsequent directional ET (Fig. 2).[2,62,63,66] An additional benefit of MOFs stems from their tunability as various organic linkers and inorganic metal nodes, which could be combined, resulting in materials with different dimensionalities. Due to the significant role of porphyrin-like

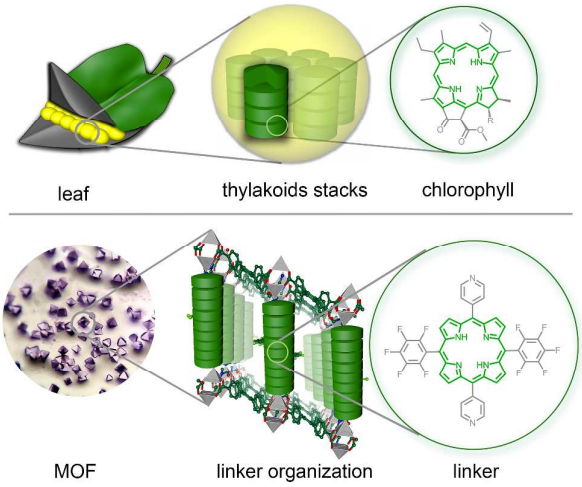

Fig. 2 Hierarchical organization of the chlorophyll molecules (*top*) and light-harvesting linkers (*bottom*) in the natural photosystem and MOF, respectively.

pigments in the process of natural photosynthesis, investigation of porphyrin-based MOFs has initially attracted attention for the development of efficient light-harvesting systems (Fig. 3).

The main requirement for a system possessing efficient light capture is its wide absorption profile ideally covering the whole solar spectrum. Therefore, establishing the communication principles between, for instance, porphyrin-based chromophores within extended ensembles such as MOFs, is absolutely crucial for improvement and tunability of their light-harvesting properties.

One of the first examples of MOFs, capable of collecting most of the light in the visible spectrum, contains porphyrin- and boron dipyrromethene-based (BODIPY) linkers.[71] The BODIPY linker served as an antenna for the excitation of porphyrinic units with subsequent exciton migration. The fluorescence quenching studies suggested that within one lifetime (~3 ns), exciton migration occurs through up to ~3 and 45 porphyrin struts inside F- and DA-MOFs,[71] respectively. This efficient exciton migration has high anisotropy along a specific direction and occurs between adjacent porphyrin struts (not in intra-layers' direction).

QDs could also be considered as promising candidates for improvement of MOF light-harvesting properties due to their wide absorption bands (Fig. 3).[74] This route was applied for modification of the mentioned DA-MOF and F-MOF with CdSe/ZnS core-shell QDs.[82] This strategy resulted in preparation of a QD-MOF hybrid possessing a broader spectral

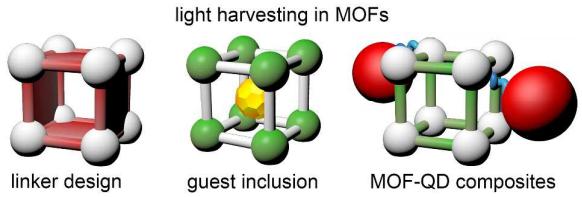

Fig. 3 Approaches for the enhancement of light-harvesting properties of MOFs. Yellow and red spheres represent the guest and QDs, respectively.

region beyond the absorption capability of the MOF itself. Thus, the QD-MOF hybrid materials are capable of capturing 50% more photons than the parent MOF. Deep and co-workers continued this direction by developing a CdTe/NTU-9 (NTU = Nanyang Technological University) composite possessing a much broader absorption profile in comparison with unmodified NTU-9.[83] The CdTe/NTU-9 composite demonstrated rapid photodegradation activity for Rhodamine 6G and an enhanced power conversion efficiency as a photoanode in a QD-dye sensitized solar cell (QD-DSSC).

Another strategy to increase overall absorption of MOFs is incorporation of molecular sensitizers inside framework pores (Fig. 3). Owing to the great capability of encapsulating various species, MOFs can be functionalized with a wide range of sensitizers, which can lead to the precise tuning of absorption properties. Yu and co-workers showed the correlation of the MOF absorption profile with the amount of positive charge on the dye molecule while encapsulated inside an anionic framework (Fig. 4).[84]

Despite the intriguing preliminary results and great potential to improve light-harvesting properties through the design of new organic linkers, and incorporation of QDs or other guest molecules, many fundamental questions in this area are still largely unexplored. For instance, the relationship of MOF topology and possible ways of exciton migration is still unknown, despite its potentially important role for the performance of sensing devices.

MOF-Sensors Coupled to ET

ET in a predesigned pathway is gaining increasing attention due to its crucial role in a wide range of applications, including sensing.[63] ET-based sensing in MOF materials could give more accurate and ratiometric detection compared to a single component system due to possibility of different ET pathways, which could occur inside one framework. MOF-based ET systems have already been explored as temperature,[36,41,75] anion, or explosive sensors.[3]

In general, ET is highly dependent on mutual chromophore organization, which is also crucial for modeling of long- and short-range ET processes. Among the few approaches to manage a large array of chromophores, self-assembly comes to forefront. Taking into account both aspects, MOFs could be considered as an ideal platform to study ET processes, particularly due to the well-defined structures of frameworks and unprecedented modularity. The latter opens different opportunities to study ET pathways including ligand-to-ligand, metal-to-metal, metal-to-ligand (or ligand-to-metal), and guest-to-MOF (Fig. 5).[61,65,85] Thus, MOFs have an unrevealed potential to help in answering the fundamental questions regarding ET principles. For instance, the MOF crystalline nature allows for the determination of distances and angles between chromophores as well as their molecular conformations by X-ray crystallography. Therefore, MOFs can be utilized as a platform to establish a necessary structure-property relationship. Incorporation of aromatic molecules as organic linkers inside a framework not only allows achievement of different packing motifs (e.g., not observed in the solid state) but also can change the nature of chromophore interactions, disturbing strong electronic coupling between molecules. One of the examples demonstrating this concept was shown by Klosterman and co-workers,[86,87] in which the incorporation of anthracene, acridine, carbazole, and naphthalene-based derivatives inside the MOF led to a unique packing motifs (i.e., extended face-to-face aromatic stacking vs antiparallel stacks or herringbone motifs observed in the crystals). This overlap increase between organic molecules resulted in an enhancement of the quantum yield from 4% to 11%.[87]

Another example of how MOFs can control photophysical properties of chromophores is based on incorporation of chromophores exhibiting aggregation induced emission (AIE).[88–91] These chromophores are almost non-emissive in dilute solutions but strongly emit in the aggregated state.[88–91]

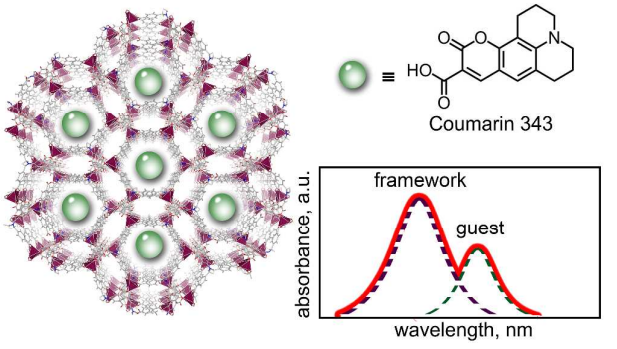

Fig. 4 Incorporation of Coumarin 343 (green spheres) inside In-based framework to enhance absorption properties of the material. The inset shows the sum of absorption profiles (solid red line) of the framework (purple dashed line, *left*) and guest (green dashed line, *right*).

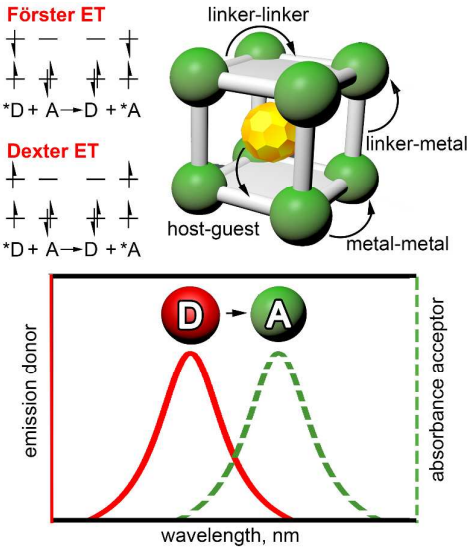

Fig. 5 (*top left*) A schematic representation of Förster and Dexter ET mechanisms. (*top right*) Possible pathways for ET in a MOF. (*bottom*) The spectral overlap of the donor emission profile (solid red line) and the absorption spectrum of an acceptor (green dashed line) required for resonance ET.

Thus, incorporation of AIE-chromophores inside a MOF matrix allowed preservation spatial separation between chromophore (similar to their behavior in solution) while maintaining their photophysical response. However, MOFs not only offer a way to restore chromophore emission but also allow utilizing such materials for sensing applications.

The first example of the MOF containing AIE-based chromophores (tetraphenylethylene (TPE)-based MOF) was reported by Dincă and co-workers.[92] They developed a "turn-on" sensor for selective detection of gaseous ammonia using temperature as a valuable parameter to achieve selectivity enhancement.[93] In this system, the analyte could bind to metals in the MOF secondary building units, and the material exhibited pore-size selectivity towards the bulkier amines. In contrast to non-coordinated pure organic linkers, which typically decompose during heating at relatively low temperature, this MOF could still maintain ligand-centered emission up to 300 °C in air, which allowed for temperature to act as a parameter for tunability of selectivity.[93] Due to this initial observation,[93] a number of the follow-up reports focusing on high-performance "turn-off" and "turn-on" TPE-based MOF sensors were developed for efficient detection of mycotoxins, benzenes, *m*-xylene, mesitylene, nitro explosives, and heavy metal ions.[88]

The other example of the MOF-based sensor is ZIF-8, which demonstrated selectivity enhancement for *n*-hexane over cyclohexane due to pore-size exclusion.[94]

Thus, all of these parameters (e.g., spatial arrangement of chromophores, their conformation, etc.) can be tuned through ligand design or reaction conditions,[63] revealing the possibility to control material photophysics (e.g., ET). In comparison with molecular complexes, where chromophores are closely packed and electronic coupling is significant, MOFs provide a pathway to achieve chromophore separation, preserving their precise organization.

Description of ET processes is reliant on coupling of two types of chromophores: donors (D) and acceptors (A). In extended architectures with weak chromophore coupling such as MOFs, ET could be mainly described using Förster and Dexter models.[63,65,66,95,96] As demonstrated in Fig. 5, Förster (or fluorescence) resonance energy transfer (FRET) works through the principle that the energy from an excited chromophore (*D), will transfer energy to a nearby chromophore (A). FRET relies on the transfer of excitation energy in a non-radiative way through Coulombic interactions between chromophores separated by 1–10 nm (Fig. 5).[95] Therefore, the emission spectrum of D must overlap with the absorption profile of A (Fig. 5). The Dexter mechanism, on the other hand, stems from intermolecular orbital overlap interactions, including electron exchange, thus occurring within a short range. In many self-assembled structures, Coulombic interactions are predominant, and ET is described in terms of the Förster mechanism.[63,96]

In the recent reports related to exciton dynamics in MOFs, a more complex mechanism is proposed.[97] In addition to the step-by-step random hopping explanation of ET, the suggested mechanism includes "through-space" jumping beyond nearest neighbors (JBNN), which should be taken into account for estimation of ET efficiency.[97] In this review, we summarized ligand-to-ligand, metal-to-ligand, metal-to-metal, and guest-to-host ET occurring in MOFs.

Ligand-to-Ligand ET

Ligand-to-ligand ET in a framework can be achieved due to the possibility to couple both D and A within a MOF. This ET pathway has been explored for a variety of MOFs consisting of, for instance, photochromic or fulleretic linkers.[98–101] In 2014, Shustova and co-workers studied ET in a MOF which was constructed from diarylethene-based derivatives (A) coordinately immobilized between porphyrin-based layers (D).[98] Due to the D-A pairing inside the framework, the photophysical properties of the host can be directed as a function of excitation wavelength, allowing for the ability of photoswitchable diarylethene-based linkers to control the photophysical response of porphyrin-containing light-harvesting assemblies.

MOFs can also be used to replicate ET pathways observed, for instance, in a protein didomain scaffold, in which chromophore cores of a green fluorescent protein variant and cytochrome b_{562} are coupled.[102–104] The choice of relevant chromophores containing hydroxybenzylidine imidazolinone (HBI) and porphyrin cores (Fig. 6) was determined by the necessary spectral overlap of the HBI derivative (D) and porphyrin-based core (A) required for FRET. Both chromophores were coordinatively immobilized in a crystalline scaffold resulting in 65% ligand-to-ligand ET efficiency.[103]

The same group also studied ligand-to-ligand ET in fulleretic MOFs containing fullerene- or corannulene-based linkers.[99,100] Fullerene (C_{60}) and its derivatives are known for their electron-accepting properties as well as ultrafast electron/energy transfer. These factors explain their widespread usage as efficient electron acceptors in organic photovoltaics[105,106] or molecular electronics.[107–110] As a small fullerene subunit, corannulene ($C_{20}H_{10}$) is much less explored than C_{60} despite its potential for effective charge

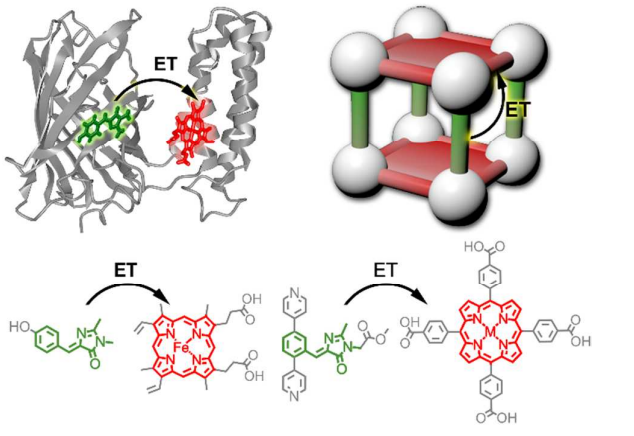

Fig. 6 (*left*) ET between two coupled chromophores of the green fluorescent protein variant and cyt b_{562} protein. (*right*) Coordinative incorporation of the chromophores with two different cores inside one framework to replicate efficient ET observed in the didomain protein system.

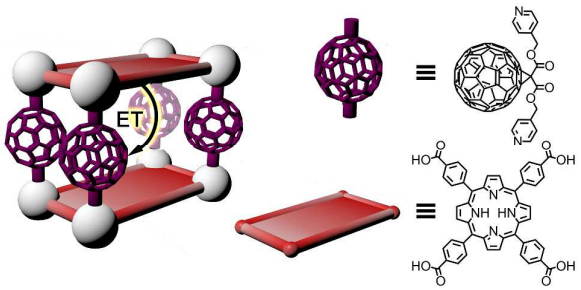

Fig. 7 A fulleretic MOF, which consists of fullerene-based acceptors (pillars) and porphyrin-containing donors (red plates).

transport.[100,111–114] In the case for the fullerene-containing linkers (A), they were immobilized between two-dimensional (2D) porphyrin-based layers (D), which the mutual orientation was controlled by metal coordination (Fig. 7).[99] For the pyridyl-based corannulene linker (D) immobilized as a pillar between 2D porphyrin-based layers (A), the ET efficiency was estimated to be 85%.[100]

Lin and co-workers developed 2D metal-organic layers (2D-MOLs) and three-dimensional (3D)-MOFs to shed light on how MOF topology could affect ET processes.[115] Although the prepared structures were constructed from the same D and A ligands, as well as metal cations (Hf), the variation of the synthetic conditions resulted in the formation of different metal node geometries and, as a result, materials with a different topology (2D-MOLs vs 3D-MOFs). After the incorporation of a second quenching ligand, the ET rates were estimated as a function of concentration of this second ligand. Quenching dynamics was estimated through the calculation of the Stern-Völmer constants, which were found to be 79.6 ± 0.3 ns^{-1} and 20 ± 2 ns^{-1} for the 3D-MOF and 2D-MOL, respectively. Due to the favorable transition dipole alignment in restricted dimensions, the donor-to-trap ET rate is faster in the 2D-MOL compared to the 3D-MOF, but the overall efficiency of ET was lower in 2D-MOLs due to slower exciton migration. Interestingly, with an external quencher (coumarin-343), the 2D-MOL had more efficient ET possibly due to a better accessibility of excitons from the external surface to the external quencher.

ET in mixed-ligand MOFs containing porphyrin- and pyrene-based ligands was studied by Lee and co-workers.[116] The coupled light-harvesting linkers possess the appropriate spectral overlap for efficient ET, which resulted in superior photoinduced singlet-oxygen generation.[116]

Recently, Lin and co-workers have devised a new concept of ET to fill in the gaps where the other models (e.g., Dexter or Förster) cannot be fully applied.[97] The exciton dynamics in MOFs are commonly described as ET between adjacent ligands in a step-by-step random hopping fashion.[61,117] Previous studies indicate nearest-neighbor hopping (NNH),[118,119] but Lin and co-workers proposed "through space" JBNN.[97] Using two light-harvesting MOFs with truxene-based ligands, it was suggested that the JBNN approach accounts for up to 67% of the ET rates.

The through-space ET concept was further studied on the example of two isostructural metal-organic layers (MOLs) with hexanuclear Zr- or Hf-secondary building units (SBUs) and a fluorescent benzene-1,3,5-tribenzote (BTB^{3-}) ligand.[120] ET was quantitatively determined through measuring fluorescence quenching after MOL doping, and through-bond or through-space ET pathways in Zr- and Hf-MOLs were studied.

Metal-to-Ligand ET

Ln-MOFs[121–123] are typical examples of systems exhibiting efficient ligand-to-metal ET. In the sensitization of Ln^{3+} ions, a photon is captured by the MOF organic linkers, then the energy is transferred to the metal ion, which results in Ln^{3+} emission (Fig. 8). For instance, Wang and co-workers showed that emission of Ln-MOFs (Ln = Eu, Tb) is a result of the highly efficient ET from the ligand to the metal centers.[124] By doping different concentrations of Eu^{3+} and Tb^{3+} ions, an emission profile of MOFs can be efficiently tuned, which could be profile of MOFs can be efficiently tuned, which could be utilized in engineering white-light emitting diodes.

Morris and co-workers studied ET processes in a UiO-67 (UiO = University of Oslo) type of a framework postsynthetically doped with ruthenium(II) bis(2,2'-bipyridine) (2,2'-bipyridyl-5,5'-dicarboxylic acid (RuDCBPY) as a function of doping degree.[125] They showed that different pathways could be responsible for ET depending on the concentration of dopant, and triplet metal-to-ligand (^{3}MLCT) excited state emission lifetime at different doping concentrations reflects the excited state deactivation. When the MOF is saturated with RuDCBPY, the quenched ^{3}MLCT lifetime is proposed due

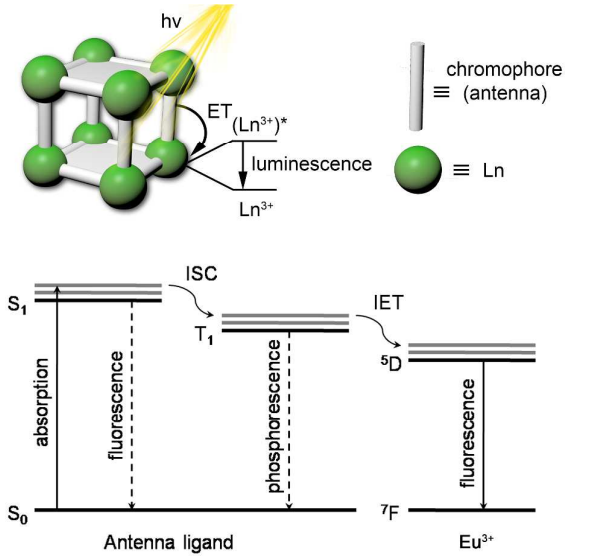

Fig. 8 (*top*) Schematic representation of the antenna effect where lanthanide ions are indirectly excited by coordinatively immobilized antenna chromophores in a MOF matrix. (*bottom*) A simplified diagram depicting the antenna effect in an Eu-based MOF. The solid arrow shows absorption of a photon followed by either fluorescence, or intersystem crossing (ISC). If ISC occurs, either phosphorescence or intramolecular energy transfer (IET) can occur, the latter will result in the emission of a photon from the Eu^{3+} species.

to Förster-type dipole-dipole 3D RET between RuDCBPY centers, but at low concentrations of the dopant, a 2D mechanism of FRET is thought to dominate the self-quenching reaction of RuDCBPY.

Metal-to-Metal ET

The Lin and Meyer research groups have pioneered investigations of metal-to-metal ET processes in MOFs.[117–119] One of possible practical applications for such metal-to-metal ET studies in MOFs could be the development of non-invasive luminescent thermometers working at a wide temperature rang This type of temperature sensing is beneficial since it does not require additional calibration of luminescence intensity and therefore, leads to more instantaneous temperature detection. For instance, mixed-lanthanide MOFs, in which Tb^{3+}-to-Eu^{3+} ET takes place, allows for the ability to tune photoluminescent properties of a framework as a function of temperature.[126] Recently, Müller-Buschbaum and co-workers studied this type of metal-to-metal ET from Tb^{3+} to Eu^{3+} on the example of a bipyridine-based MOF.[127]

Guest-to-MOF (MOF-to-Guest) ET

Porous frameworks also offer a unique opportunity to study host (MOF)-to-guest and guest-to-host ET pathways due to possibility of tuning their topology for the selective inclusion of desired guest molecules.

For instance, a high efficiency of ET (72%) was demonstrated on the example of a benzylidene imidazolinone derivative (D) incorporated inside a 3D porphyrin-based framework (A).[103,128–130] In 2014, Wang and co-workers were able to construct a two-color luminescent system (blue/red) through the introduction of 4-(dicyanomethylene)-2-methyl-6-(4-dimethylaminostyryl)-4H-pyran (DCM) inside the framework. The intensity ratio of blue to red fluorescence varies in different planes within the MOF crystal suggesting MOF-to-DCM ET.[131]

Recently, Zang and co-workers used a fluorescent $Cd_2(APT)_3(HDABCO)_2$ (APT = 2-(2-acetoxy-propionylamino)-terephthalic acid, HDABCO = 1,4-diazabicyclo[2.2.2]octane) framework to study host-to-guest'-to-guest'' ET (Fig. 9).[132] The MOF host can act as a light-harvesting antenna, and therefore, as a D in the host-to-guest' ET to acridine orange, which participates in sequential ET to Rhodamine B. Successful realization of such multistep ET was feasible due to framework tunability, which allowed incorporation of several guests possessing the necessary spectral overlap, for instance, between the MOF emission and guest' absorption, and the guest' emission and guest'' absorption.

Allendorf and coworkers utilized MOF-177 as a scaffold for incorporation of α,ω-dihexylsexithiophene (DH6T) and [6,6]phenyl-C_{61}-butyric acid methyl ester (PCBM).[85] In this case, FRET could be a possible pathway of ET between the scaffold and DH6T, while either energy or electron transfer is possible between the MOF and PCBM. The DH6T compound can have a dual role, in which it can act as an A for MOF-177 and a D for PCBM, thus promoting ET.

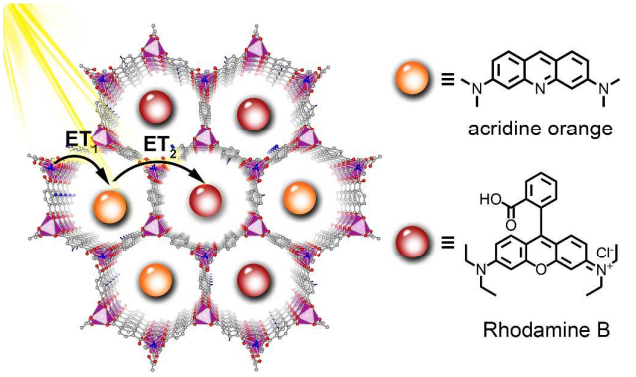

Fig. 9 Stepwise host-to-guest'-to-guest'' ET in the $Cd_2(APT)_3(HDABCO)_2$ framework with two encapsulated dyes: acridine orange (orange spheres) and Rhodamine B (red spheres). The purple, gray, blue, and red spheres as a part the MOF structure represent Cd, C, N, and O atoms. Hydrogen atoms were omitted for clarity.

As a result of continuous investigations of ET in MOFs, the first FRET-coupled MOF sensor for the detection of free bilirubin (the breakdown product of hemoglobin turnover) was reported by Jia and co-workers.[133] The concentration of bilirubin in human serum is an important parameter for diagnosis of liver disorders. The interactions of 2,3,4-trihydroxybenzaldehyde functional groups inside the pores of MOFs with free bilirubin resulted in quenching of MOF emission *via* the FRET process, allowing detection of free bilirubin by the naked eye. The developed material showed not only a fast response but also high sensitivity and selectivity towards free bilirubin molecules over other biomolecules and metal ions.[133]

To summarize, although studies of ET processes in MOFs are an emerging interest, their understanding and modeling are still a great challenge. For MOFs to be utilized in their full capacity, the gap between the structural principles and ET mechanisms should be closed. Moreover, in reference to ligand-to-ligand-ET, many examples are based on porphyrin-containing chromophores, which significantly limit MOF topology, conformation of chromophores, and material photoluminescence response. All of these restrictions also affect the overall ET efficiency. Furthermore, the guidance of ET in a predesigned pathway could be governed through chromophore organization inside the MOF structure, but its understanding is still in the rudimentary phases.

Photocatalysis as the Pathway for Subsequent Sensing

Photocatalysis could be considered as a powerful concept to enhance selectivity or lower detection limits in MOF-based sensors due to formation of new analytes, which precursors were not easily detectable before their chemical transformations. Furthermore, MOF-based photocatalysts provide a way to mediate thermodynamically uphill reactions under mild conditions, i.e., by utilization of a green chemistry approach.[134–136] The modular nature of MOFs also provides several pathways for integration of catalytically active sites and possible systematic control over the nature of these

sites.[62,65,67,76–78] Furthermore, a MOF scaffold could replicate fundamental steps required for efficient photocatalysis including light harvesting, separation and migration of charge carriers, and the initiation of redox reactions by the charge carriers.[62,65,67] In this review, we summarize the recent advances in the field of MOF photocatalysis with the exception of MOF-promoted water splitting. We will further narrow down our focus by excluding catalytically-active guests from our consideration since they were recently covered in a review by Cohen and co-workers.[137] Thus, the scope of this article covers photocatalysis performed on MOF metal nodes and organic linkers (Fig. 10).

One of main driving forces towards MOF utilization for photocatalysis relies on the possibility of multistep light-induced processes: light harvesting centered on organic linkers with subsequent catalysis on homogeneously distributed catalytically active sites. MOFs can be considered as an array of different types of catalysts located on different parts of a framework: metal nodes, organic linkers, and encapsulated guests. Each catalytic site can operate individually or form an "alliance" with another type of a catalytic center. Such cooperative effect of multiple active sites may potentially be applied towards tandem catalysis. In addition to advantages inherent to heterogeneous catalysts such as facile product separation and catalyst recovery, MOF pores can restrict the spatial reactant-catalyst alignment, which could lead to different reaction pathways and alternative products not accessible with "conventional" catalysts. To date, photoactive MOFs were applied for a number of organic transformations, including, for instance: (**1**) oxidation of alcohols, amines, alkene, alkanes, and sulfides; (**2**) C–H bond activation, or (**3**) atom-transfer radical polymerization (ATRP).[137] We structure our review based on the nature of the photocatalytic centers: metals (inside SBUs or chelating to organic ligands) and linkers suitable for organocatalysis.

Ti-MOFs

Among many popular photocatalysts, titanium dioxide (TiO_2) is one of the most widely investigated semiconductors for a variety of photoreactions, due to its wide absorption profile and high oxidation potential.[138–142] Therefore, it is logical to suggest that the possible organization of Ti-based oxoclusters inside a framework will be of great interest to the photocatalysis community. Furthermore, spatial separation of Ti-oxo-SBUs allows one to solve a problem associated with a low surface area of nanoparticles as well as their sintering. Therefore, in combination with large surface area and high porosity, the development of Ti-based MOFs represents a next step in the development of Ti-based photocatalysts.[143] The crystalline Ti-based MOF, MIL-125 (MIL = Materials Institute Lavoisier), exhibited photocatalytic activity in an alcohol oxidation.[144] In this case, irradiation with UV light promotes the alcohol oxidation (e.g., methanol, ethanol, or benzyl alcohols) concomitant with formation of Ti(III)-Ti(IV) species. The computational studies performed by Walsh showed that it is plausible to tune the optical response of the Ti-based MOFs through organic linker functionalization.[145] For instance, different substituents on the BDC^{2-} (BDC^{2-} = benzene 1,4-dicarboxylate) core can change the valence band from 3.5 eV to 2.4 eV. In addition, incorporation of a BDC-$(NH_2)_2^{2-}$ linker could shift the absorption profile into the visible region.

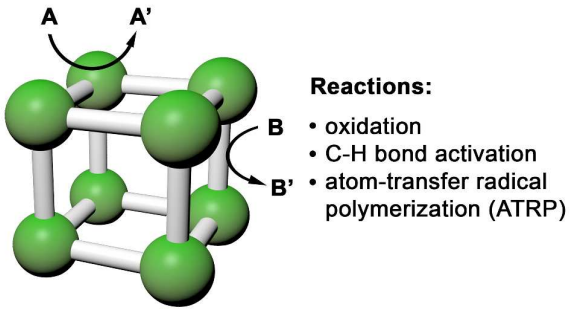

Fig. 10 Photocatalysis in MOFs occurring on metal nodes (A -> A') and organic linkers (B -> B').

The catalytically active NH_2-MIL-125(Ti) was investigated by Li and co-workers for reduction of CO_2 to formate, as well as aerobic oxidation of amines to the corresponding imines; the latter ones are important building blocks for preparation of pharmaceuticals.[146] To evaluate the influence of aminated linkers to photocatalysis, Mellot-Draznieks and co-workers prepared a series of mixed-linker MIL-125-NH_2-MOFs containing different ratios of BDC^{2-}/BDC-NH_2^{2-} ligands.[147] The maximum catalytic activity for benzyl alcohol oxidation is reached in the case of 50% of BDC-NH_2^{2-} incorporation. Thus, aminated linkers were shown to improve the optical absorption profiles, however, no correlation with the amount of incorporated BDC-NH_2^{2-} was reported.

Recently, Ti-based MOFs (MOF-901 and MOF-902) outperformed the photocatalytic activity of the commercially available P25-TiO_2 in the polymerization of methylmethacrylate under visible light.[148,149]

Fe-MOFs

Since iron is one of the earth abundant metals, Fe-based MOFs could be a logical choice for the next generation of equally effective and inexpensive heterogeneous catalysts.[150] In 2015, two water-stable Fe-based MOFs, MIL-100(Fe) and MIL-68(Fe), were used as photocatalysts to perform selective benzene hydroxylation using hydrogen peroxide as an oxidant.[151] The benzene conversion was found to be 20% and 14% by the use of MIL-100(Fe) and MIL-68(Fe), respectively. In the case of both photocatalysts, reaction selectivity reaches 98%. Thus, these examples demonstrate a more cost efficient, green route for phenol production. Another example of the MIL family, NH_2-MIL-101(Fe), has been applied in a photocatalytic reaction between aromatic alcohols and active methylene compounds, such as ethyl cyanoacetate or diethyl malonate, in a tandem photo-oxidation/Knoevenagel condensation using visible light.[152] The framework itself not only acts as the photocatalyst for alcohols-to-aldehyde

oxidation, but also as the base catalyst for the Knoevenagel condensation, highlighting MOF multifunctionality.

Metalloligands in Ru- and Ir-MOFs

Utilization of catalytically-active linkers is an attractive strategy to create photoactive MOFs. Over the last decade, $Ru(BPY)_3$ (BPY = 2,2′-bipyridine) and similar complexes have been shown as efficient photocatalysts for organic transformations including [2+2] cycloadditions,[153] α-alkylation of aldehydes,[154] aza-Henry reactions,[155] aerobic amine couplings,[156] hydroxylation of arylboronic acids,[157] or sulfide oxidations.[158] In 2011, Lin and co-workers incorporated polypyridyl Ru(II) and Ir(III) complexes into the UiO-67 MOF to study photocatalytic organic transformations including the aza-Henry reaction, aerobic amine coupling, and aerobic oxidation of thioanisole.[159] Following the inspiration from this work, Cohen and co-workers incorporated a Ru-based complex into the UiO-67 MOF through postsynthetic modification (PSM) for the aerobic oxidation of arylboronic acids under irradiation with near-UV and visible light.[160] Through changing the PSM reaction time, the degree of ruthenium incorporation could be tuned from 2 to 15%. In the case of aerobic oxidative hydroxylation of arylboronic acids using UiO-67-$[Ru(BPY)_3]_{0.1}$, the overall reaction yield of 81% is only slightly less than that of the homogeneous reference system ($Ru(BPY)_3Cl_2$). In 2016, Cohen and co-workers extended the utilization of the PSM strategy towards integration of Ir(III) polypyridyl complexes into the same MOF, UiO-67, to photocatalyze the 2,2,2-trifluoroethylation of styrenes. The catalytic activity was preserved at least for the first three initial catalytic cycles.[161] Furthermore, the prepared Ir(III)@UiO-67 catalyst showed better selectivity for the desired hydroxytrifluoroethyl products than its homogeneous Ir(III) analogs, highlighting the crucial role of the "pore confinement effect" for suppression of by-product formation.

Metallated Porphyrins in In- and Sn-MOFs

Metalloporphyrins could be considered as a special and well-studied class of metalloligands.[162–166] The high tunability of MOFs provides several ways for metal incorporation inside the porphyrin core: pre-metallation,[82,167,168] *in situ* metallation,[71,169,170] postsynthetic cation exchange,[171] or complete replacement of a non-metallated linker with a metal-containing one using solvent-assisted linker exchange.[172]

In 2014, Zhang and co-workers reported a controllable *in situ* metalation of an anionic porphyrin-containing In-MOF (UNLPF-10, UNLPF = University of Nebraska–Lincoln porous framework), where the extent of metalation in the porphyrin macrocycles was tuned through varying the indium to ligand ratio.[173] The photosensitizing capability of the indium-metaled porphyrin macrocycle was used to study photocatalytic activity of UNLPF-10 in regard to the selective oxygenation of sulfides. For example, thioanisole was completely and selectively converted to sulfoxide in 8 hours. The conversion after five cycles of a photo-induced oxidation using UNLPF-10 was found to be 97%. The photo-oxygenation rate of thianosole was shown to be dependent on the amount of metallated porphyrin sites. For example, over 40 hours are necessary to achieve full conversion through the use of UNLPF-10 with 25% of In-sites, while only 8 hours was necessary to achieve the same result using the MOF containing 98% of In-sites. Moreover, the prepared framework showed enhanced photocatalytic activity for photo-induced oxidation of sulfides in comparison with its homogeneous analog, tetraphenylporphyrin, or its In-containing derivative.

In a follow-up paper, Zhang and co-workers continued their investigation of catalytic activity of porphyrin-based photoactive MOFs as a function of metal inside the porphyrin macrocycle.[174] On the example of the mentioned above In-MOF, UNLPF-10, they prepared four isostructural MOFs with different high valent metal centers (In(III), Sn(IV)) and showed their catalytic activity towards three organic reactions, such as aerobic hydroxylation of arylboronic acids, oxidative primary amine coupling, and the Mannich reaction.

Photo-induced oxidation of sulfide and phenol was studied by Wu and co-workers using a MOF containing tin (IV)-porphyrin linkers.[175] Photo-oxidation of sulfides catalyzed by the MOF resulted in reaction yields as high as >99%, and was found to be more efficient than that of its corresponding component $Sn^{IV}(OH)_2TPyP$ (TPyP = 5,10,15,20-tetra(4-pyridyl)porphyrin).

Photo-organocatalysis

Utilization of chromophores for photoorganocatalysis has already been proven as an emergent area of research.[136,137,176–180] However, merging advantages of light-harvesting chromophores with benefits offered by a MOF platform, such as porosity, modularity, tunability, high surface area, and crystallinity is only studied to a small extent as highlighted by the few examples below(Fig.11).

The photoactive MOF (NNU-35, NNU = Northeast Normal University) was probed towards efficient ATRP (Fig. 11).[181] The anthracene-based bipyridine ligands and terephthalate linkers were integrated within one framework resulting in preparation of the photosensitizer (PS), NNU-35, possessing a broad absorption profile. The polymerization process was based on the reduction of the Cu-based complex present in the reaction mixture by electron transfer from NNU-35. The produced polymers were characterized by a narrow molecular weight distribution. However, a relatively low conversion observed in these reactions is still an ongoing challenge, which may be potentially resolved through the optimization of reaction conditions (e.g., temperature).

Another example of organocatalysis was demonstrated on a MOF constructed from TPE-based linkers (Fig. 11).[89,93,182] The prepared MOF exhibited a high photocatalytic activity in aerobic cross-dehydrogenative coupling (CDC) reactions under irradiation with visible light. Moreover, yields of the CDC reactions between substituted tetrahydroisoquinoline derivatives and nucleophilic indoles surpass 85%. Mechanistic studies confirmed the crucial role of molecular oxygen in these

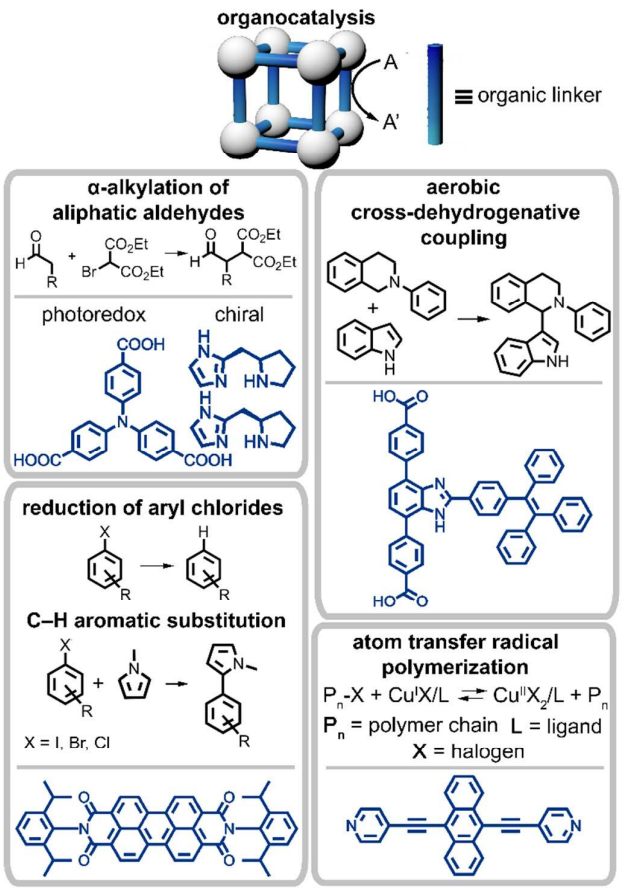

Fig. 11 Organophotocatalysis on photoactive MOFs depicting general scheme of organic transformations (black) and photoactive organic linkers (blue); (*top left*) α-alkylation of aliphatic aldehydes, (*top right*) aerobic cross-dehydrogenative coupling, (*bottom left*) reduction of aryl chlorides and C–H aromatic substitution, and (*bottom right*) atom transfer radical polymerization.

aerobic reactions, which is in line with the fact that under a nitrogen atmosphere, no product formation was observed.

Duan and co-workers used the tunable nature of MOFs to integrate different types of active centers within one framework to catalyze the *α*-alkylation of aliphatic aldehydes (Fig. 11).[183] Through the integration of pyrrolidine-2-ylimidazole (PYI)- and triphenylamine (TPA)-containing photoactive linkers within one structure, chiral Zn-MOFs were prepared. The synergistic effect of the two linkers resulted in high enantioselectivity: the photoactive TPA-based linker in the excited state induced electron transfer to form an active intermediate for α-alkylation, while the chiral PYI-based linker acted as an asymmetric catalyst to achieve stereoselectivity. Control experiments clearly demonstrated that the presence of both linkers is essential to achieve a reaction yield of 74% and an enantioselectivity of 92% *ee*. This work demonstrated the unrevealed potential of MOFs towards tandem catalysis through integration of several independent catalytic sites within one platform.

The Hupp and Farha research team demonstrated a different approach for incorporation of photocatalytically active linkers inside a framework.[184,185] They postsynthetically incorporated different PSs (e.g., [6,6]-Phenyl-C_{61}-butyricacid (PCBA) or BODIPY derivatives) into a Zr-based MOF for selective oxidation of a sulfur mustard simulant.

In the photocatalytic reduction of aryl halides, Duan and co-workers utilized the idea of consecutive photoinduced electron transfer through the incorporation of a perylene diimide (PDI) derivative inside the MOF (Fig. 11).[186] For the test reactions: reduction of aryl chlorides, C–C bond formation through coupling between aryl chlorides and N-methylpyrrole, photooxidation of benzyl alcohol, and oxidative coupling of amines were investigated. In many cases, enhancement of catalytic performance was observed in comparison with non-coordinated PDI-based molecules.

As shown in the section above, the amount of MOFs able to perform photocatalytic organic transformations is continuously increasing. The MOF pores can act as molecular sieves to separate reagents and products based on their sizes with their further detection by specific interactions of these guest molecules with the framework. Such a concept could serve as a foundation for photoinduced sensing. In order to build such sensor materials, a deeper understanding of the interactions of guest molecules with a framework scaffold is necessary, as well as a multi-step design of frameworks for incorporation of photoactive units capable of sensing at the same time. Currently, there are no examples of MOF-based sensors directly coupled to photocatalytic organic transformations. However, Jiang and co-workers presented a porphyrin-based MOF capable to catalyse the Heck reaction after the addition of copper solution as a trigger for sensing.[187] The presented MOFs serve as a "turn-on" sensor for Cu^{2+} ions, which involved the following steps: (i) replacement and release of Pd^{2+} ions from the porphyrin core of the linker upon addition of copper solution; (ii) reduction of the released Pd^{2+} ions to Pd nanoparticles; (iii) conversion of nonfluorescent aniline to fluorescent indole in the Pd-catalyzed Heck cross-coupling reaction. Thus, the presence of Cu(II) ions was detected based on enhancement of the fluorescent signal from the presence of a emissive reaction product. The presented system shows the possibility to couple catalytical performance with sensing ability inside one MOF platform.

Singlet Oxygen for Analyte Detection

There are a number of applications dependent on efficient singlet oxygen ($^1O_2$) generation.[188] One of them is photodynamic therapy (PDT), which is a rapidly developing area for utilization of MOFs focusing on induction of abnormal cell death (e.g., cancer cells).[189] However, *in situ* generated $^1O_2$ could be utilized for selective oxidation, which opens a pathway to monitor product formation (or reactant disappearance), which could lead to sensor development coupled to $^1O_2$ generation. Especially, in addition to tunability and porosity, necessary for sensing, the well-defined nature of MOFs is advantageous for singlet oxygen production since it aids in precise spatial control over the PS assembly and impedes self-quenching of the excited states.[188,190]

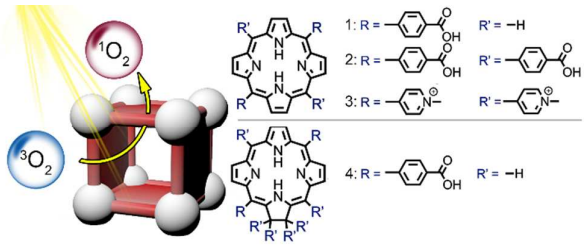

Fig. 12 Singlet-oxygen generation using porphyrin-based organic linkers in a MOF.

The combination of thermal and chemical stabilities and photosensitizing properties make porphyrin-based linkers one of the most commonly used building blocks for construction of MOFs for $^1O_2$ (Fig. 12). For instance, Lin and co-workers demonstrated that the porphyrin-containing Hf-MOF could promote intersystem crossing to increase the number of reactive oxygen species as well as faster diffusion of $^1O_2$ through the pores.[190]

An example of a "porphyrin-free" MOF applied towards $^1O_2$ production was developed by Wang and co-workers in 2016 through the incorporation a non-porphyrin PS (BODIPY) in the UiO-type MOF.[191] The prepared UiO-BODIPY framework demonstrated the enhancement of BODIPY photostability in comparison with the free ligand,[191] however, the ability to generate $^1O_2$ does not surpass that of the linker itself.

To summarize, the discussed results demonstrated that MOFs could be a very promising platform for singlet oxygen production, which in combination with other advantages offered by a MOF, could be applied for efficient monitoring of product formation or degradation. The latter fact outlines an unrevealed impact for the field of MOF-based sensors.

Sensors "on Demand"

The potential to change the properties of MOFs as a function of external stimuli could be utilized for development of not only the next generation of lenses or "smart windows", but also sensors.[192–197] One of possible pathways to engineer photoresponsive sensors is through the integration of photochromic compounds inside a MOF matrix (Fig. 13).[197] Photochromic compounds are able to switch between two discrete states upon, for instance, irradiation.[192,198–204] Thus, they can be used as a switch to control physicochemical properties of frameworks.[192,198–204] Moreover, integration inside a framework could lead to a solution of a commonly occurring problem observed for many photochromic molecules: their restricted photoisomerization in the solid state.[205,206] Integration of photochromic materials with porous MOFs could lead to a solution of this problem due to spatial separation of photoswitchable molecules inside a MOF. In general, photochromic sensors have a number of advantages in comparison with "conventional" ones including (i) multiple signal outputs and therefore, more information for analysis, (ii) recognition can be tuned as a function of photoisomerization, which also provides a pathway to bind several analytes simultaneously, and (iii) isomerization and therefore, sensing ability can be controlled not only by the excitation wavelength, but also by electric field, temperature, or pH. To achieve benefits offered by photochromic sensors, the first step is their integration inside a MOF. In this review, we will focus on integration of spiropyran-, diarylethene-, and azobenzene-based compounds inside a framework (Fig. 13).[69,192,198–204] Azobenzene and its derivatives are known to undergo large structural changes during photoisomerization, while they only have small differences in absorption spectra, unlike diarylethene that not only undergoes structural

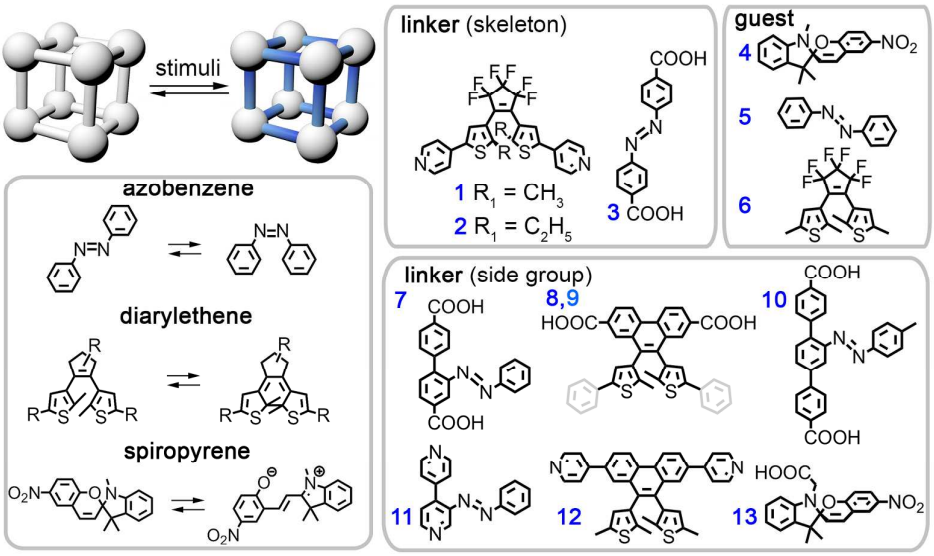

Fig. 13 Preparation of photoresponsive MOFs through coordinative immobilization of photoswitchable organic linkers as a framework backbone or a side group, as well as non-coordinative immobilization.

transformations, but also has distinct absorption profiles for the two isomers, detectable by the naked eye. Spiropyran undergoes a large structural change upon a ring opening event, which is triggered by UV light (Fig. 13).

There are two main approaches for incorporation of photoresponsive units inside MOFs: linkers and guests. Linkers can contain the photoswitchable part as (i) a main part of their backbone and (ii) as a side group located in the pores of the framework which does not interfere with the rigid component of the ligand (Fig. 13). It is logical that the photoswitchable linkers that undergo structural changes along their backbone will behave differently than linkers with the photoswitchable group oriented towards the pore. The latter ones will have more freedom for photoisomerization, and the difference between these two approaches will be highlighted in the context of this review.

Photochromic Compounds as a Framework Backbone

In order to incorporate photochromic compounds where isomerization occurs through the backbone of the structure, it is crucial to maintain framework flexibility to handle the structural transformations of the photoswitch. In addition to structural considerations, one of the main challenges, though, with incorporation of photochromic ligands as a backbone of a MOF is the quantitative reversible photoisomerization of the photoswitch. Kitagawa and co-workers developed a strategy of how to overcome this drawback through the synthesis of an interpenetrated diarylethene-containing framework.[207] They designed a framework which has enough degrees of structural flexibility to accommodate changes after photoisomerization, which was confirmed by single crystal X-ray diffraction. A 3D interpenetrated structure was obtained by incorporation of a diarylethene-based derivative (**1**, Fig. 13) between 2D layers of a non-photochromic framework. The interpenetrated structure allows for changes in linker geometry without framework collapse. In addition to X-ray diffraction analysis, linker photoisomerization was also confirmed by spectroscopic studies, as well as CO_2 sorption measurements, showing the possibility to tune the void space inside the framework. A similar approach was utilized by Barbour and co-workers, who confirmed that the degree of framework penetration influences the photophysical response of the incorporated photochromic linker (**1** and **2**, Fig. 13).[208]

Luo and co-workers reported preparation of a photoactive MOF with the ability to control catalytic processes upon exposure to an external stimulus.[209] An azobenzene-based derivative suitable for MOF preparation (i.e., azobenzene core functionalized with carboxylate groups) was used as the organic linker. The resulting MOF (ECUT-50, ECUT = East China University of Technology) possesses one-dimensional channels offering selectivity in catalysis through the confined spaces within the MOF pores. ECUT-50 was probed as a heterogeneous catalyst for a Knoevenagel condensation, a common base-catalyzed reaction, due to the basicity of the –N=N– group in azobenzene. As a result, high size-selectivity was achieved. Moreover, ECUT-50 was found to be inactive upon UV irradiation for the Knoevenagel condensation, confirming the idea of photoswitchable catalysis. A dynamic framework that showed light-induced structural flexibility was prepared by Hill and co-workers.[210] In this report, a photoactive azobenzene-based derivative (**3**, Fig. 13) was combined with a trans-1,2-bis(4-pyridyl)ethylene linker.[211] The resulting framework was able to accommodate structural changes and showed oscillating behavior between the two isomeric forms for both incorporated linkers under irradiation with two different excitation wavelengths. This light induced structural flexibility could be applied for controllable CO_2 capture and release.

Recently, Luo and co-workers combined two photochromic linkers (azobenzene- and diarylethene-derivatives) (**1** and **3**, Fig. 13) into a single Zn-based MOF (ECUT-30) as a way to control the adsorption selectivity by irradiation with light.[212] The ECUT-30 MOF has considerable adsorption capacity towards CO_2, C_2H_2, and C_2H_4, alongside distinct photoresponses towards different guest molecules.

Photochromic Unit as a "Side Group" of the MOF Linker

As discussed above, isomerization of photoswitchable linkers within a framework typically may result in significant structural changes, which in many cases cannot be accommodated without framework decomposition. Functionalization of the organic linker backbone with a photoresponsive side group is a more feasible approach to preserve MOF integrity. To date, this approach was mainly studied to modulate the storage properties of MOFs for a number of guests (e.g., CH_4, CO_2, or dyes).[213]

One example of optically induced changes in the storage properties of MOFs was shown by Zhou and co-workers.[214] They utilized 2-(phenyldiazenyl)terephthalate (Fig. 14) as an organic linker decorated with a photoswitchable side group to build the framework. Although, they did not perform any spectroscopic studies to show the isomerization of an

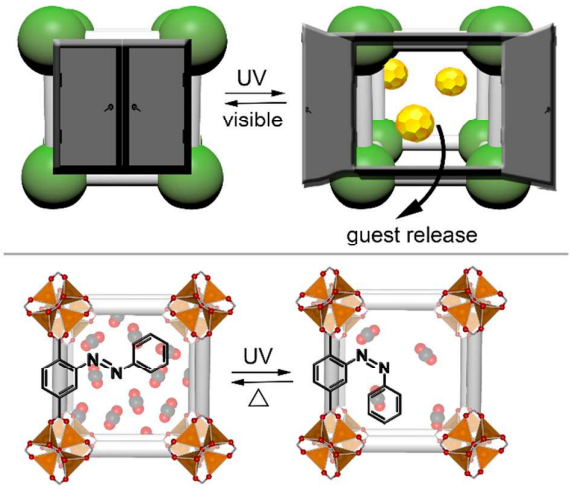

Fig. 14 (*top*) Light-induced guest release in MOFs with photochromic linkers. (*bottom*) Light-induced release of carbon dioxide achieved through azobenzene linker isomerization.

azobenzene derivative, they demonstrated the possibility to control CO_2 uptake upon irradiation with light. The spectroscopic and theoretical calculations on the could take place inside the pores. In the two different MOFs, photoswitching was only enabled in one MOF structure, while in the other, the presence of a second linker was blocking the trajectory of photoisomerization. This work showed the possibility to control photoisomerization through utilization of MOFs, which can be further supported with theoretical calculations.

Photoisomerization of organic linkers inside the framework could potentially lead to tunability of material properties by changing the excitation wavelength. For instance, the proof of concept for on-demand drug release was shown on the example of a biocompatible Zr-MOF, in which the organic linker was functionalized with an azobenzene group (**10**, Fig. 13).[216] The pores of the framework were capped through binding with ß-cyclodextrin decorated with azobenzene derivatives, allowing to trap compounds of interest inside a MOF. This supramolecular complex can dissociate under light, leading to release of trapped molecules. The presented approach shows the possibility of MOF utilization for applications in light-induced drug release where no additional chemical components are necessary.

Introduction of spiropyran-based derivatives inside the framework structure is still a remaining challenging due to the high degree of structural changes of the photoswitch molecules during photoisomerization. D'Allesandro and co-workers showed a novel approach for incorporation of photochromism into MOFs through a two-step PSM of metal clusters (**13**, Fig. 13).[217] The ability of the spiropyran-derivative attached to a metal node to isomerize inside the framework pores was shown in their photophysical studies. UV-irradiation resulted in stabilization of the open merocyanine form, which was attributed to its stabilization by the presence of polar Zr-OH groups in Zr-based metal nodes. Additionally, a further increase in temperature does not show the expected relaxation of merocyanine back to spiropyran, which supports the idea of stabilization of the polar form through the polarity of framework cavities.

Although incorporation of a photochromic core as a side group of the linker backbone is seen as a promising strategy to facilitate photoisomerization, the MOF matrix can alter the known behavior of photoswitches in an unpredicted way. This approach can be utilized as a new way to introduce additional functionality to known MOF topologies. Benedict and co-workers reported a series of diarylethene-based MOFs where a diarylethene group was placed inside the pores of the framework (**8**,**9**, and **12**, Fig. 13).[218] In the first step, through synthesis of the dicarboxylate diarylethene-containing MOF, they showed changes in the photophysical behavior in comparison to solution studies. While the prepared photochromic linker undergoes reversible isomerization in solution, it was no longer reversible after its incorporation inside the framework. The observed changes in behavior were attributed to changes in the linker environment and possible stabilization of the colored form of the photoswitch by the framework. To further study the effect of the framework on the photoisomerization of diarylethene derivatives after their coordinative immobilization, the diarylethene core was decorated with bulkier phenyl groups instead of methyl groups (**9**, Fig. 13).[219] This modification again resulted in changes of photoisomerization behavior inside the framework in comparison to that in solution. However, in this case, the observed variations were not explained by changes in the microenvironment of the photoswitch, but by stabilization of the photoinactive orientation of the side groups inside the pores of framework. In the most recent report by the same group, the backbone of the linker was extended by pyridyl groups (**12**, Fig. 13), and the final organic linkers were used as pillars between 2D layers. This approach allows for the increased spacing between photoactive groups, which could facilitate their photoisomerization inside the pore space.[220] Unfortunately, it again resulted in a non-reversible behavior of the diarylethene group due to significant structural reorganization upon irradiation.

Photochromic Compounds as Guests inside MOF Pores

As a way to overcome the spatial confinement of solid-state photoswitches, non-coordinative inclusion could be applied. In a recent study, Ruschewitz and co-workers loaded a photoswitchable spiropyran-based molecule (**4**,Fig. 13) into the pores of various MOFs (MOF-5, MIL-68(In), and MIL-68(Ga)), in order to shed light on how the host (MOF) affects the optical properties of the guest (spiropyran derivative).[221] The incorporated guest into the aforementioned MOFs exhibits behavior observed in solution rather than in the solid state.

Photoswitchable guest molecules were also shown to trigger structural transformations of a host framework as studied by Kitagawa and co-workers.[222] An azobenzene molecule (**5**, Fig. 13) was introduced into the pores of a flexible Zn-based MOF ($[Zn_2(terephthalate)_2(triethylenediamine)]_n$), where *cis*/*trans* isomerization of the guest was studied. This photoisomerization, induced by light or heat, resulted in the reversible structural transformations of the host from the initial tetragonal crystal system to an orthorhombic one. The changes observed in the host structure were also dependent on the ratio of the isomers incorporated inside the pores. Despite the reversible isomerization of azobenzene inside the framework pores, the activation energy for this conversion was much higher in comparison to solution behavior. The same Zn-based MOF was utilized by Benedict and co-workers for incorporation of diarylethene-based guest molecules (**6**, Fig. 13) to study their photoisomerization inside the flexible host.[223] In this study, a change in absorption profile was observed upon UV irradiation, which could be reverted back upon irradiation with visible light, allowing an "on and off" switching potential. Interestingly, the polarized absorption spectra showed linear dichroism in the obtained guest@MOF system, confirming not only inclusion of the guest molecules, but also their preferential alignment within the pores of the host.

MOFs as a Tunable Nanoreactor

Due to unprecedented modularity and versatility, MOFs are gaining increasing interest as "tunable nanoreactors". Such "reactors" could completely change the reaction outcome in comparison with the same reactions in more conventional "flasks" due to the fact that confined space could influence the arrangement of encapsulated guests, and therefore, significantly affect their interactions.[224–228] In the scope of this review, we want to describe two potentially useful concepts for novel MOF-based sensors which rely on (i) sensing of the products, formation of which occurs due to the confining nature of MOF nanoreactors and (ii) sensing of emissive products produced from non-emissive reagents inside the MOF scaffold. In the first case, a MOF will serve as a "reaction vessel" providing a spatial confinement for selective product formation, which sensing will occur through a change of the MOF photophysical response (Fig. 15). The second case relies on the appearance of product emission due to suppression of low energy vibrational modes because of integration inside the MOF pores. Even though there are no literature precedents of such systems for MOFs yet, a number of supramolecular systems discussed below could be used as initial steps to demonstrate the feasibility of the proposed concepts. For instance, various supramolecular containers, which could facilitate unusual chemical reactivity or promote specific reactions, have been reported.[229,230] For instance, trans-1,4-polyisoprene could be formed with a high selectivity upon isoprene photoirradiation inside the confined environment of pyridyl-phenylethynylene bis-urea macrocycles under mild conditions.[229] In addition to easy polymer release, this crystalline host is reusable. Another example, which demonstrated advantages of a confined space, is photodimerization investigated by Fujita and co-workers in self-assembled coordination cages.[230] Using a cage, assembled from metal ions and tridentate ligands, they showed that acenaphthylenes (or naphthoquinones) could be selectively encapsulated followed by [2+2] photodimerization. In this case, the cage cavity could accelerate the speed of the reaction and control the stereochemistry of the product.[236] These supramolecular precedents demonstrate a significant potential and possible impact of a "nanoreactor" geometry and dimensions on a number of chemical transformations, but from the perspective of this review, provide an intriguing hint for porous and modular structures of MOFs to be used in sensing applications. Very recently, a study shed light on the possibility for applying the same concepts by the utilization of MOF pores. For instance, MOF-74[231] could be utilized as a "smart "nanoreactor" for the storage and photoinduced release of uranyl ions.[232] In this case, the encapsulated coumarin molecules were able to undergo photoinduced dimerization inside porous of a framework and acted as a controlled gate for storage and release of uranyl ions (Fig. 16).[232] Tracking such release or storage by photoluminesce spectroscopy (e.g., through changes of the MOF emission profile or through emission of uranyl ions) foreshadow the utilization of MOFs not only as useful nanoreactors, but also as sensors offering potential benefits including pore-shape (or size) selectivity and wall multifunctionality.

In 2010, Kitagawa and co-workers introduced a novel concept of photoactivation of the pores' surface.[233] A photoresponsive nanoporous framework functionalized with aryl azide group was developed, which could be converted to nitrenes after irradiation with UV light.[233] This approach can open a novel path for the functionalization of pore surfaces of MOFs, leading to the potential use for recognition of different types of molecules or for controlled chemical reactions.

To summarize, MOFs have an unexplored potential to be utilized as "tunable nanoreactors" in sensing applications, which could provide a foundation for the development of first examples of efficient "reactor-sensor" couples.

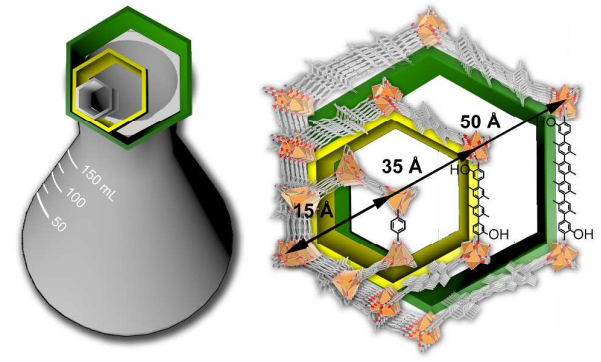

Fig.15 Schematic representation of MOFs as nanoreactors.

Conclusion and Perspectives

As highlighted in this review, MOFs have the potential to move beyond the pore exclusion approach for development of new sensing devices. Recent advancements in the fields of MOF photophysics and photochemistry foreshadow that light

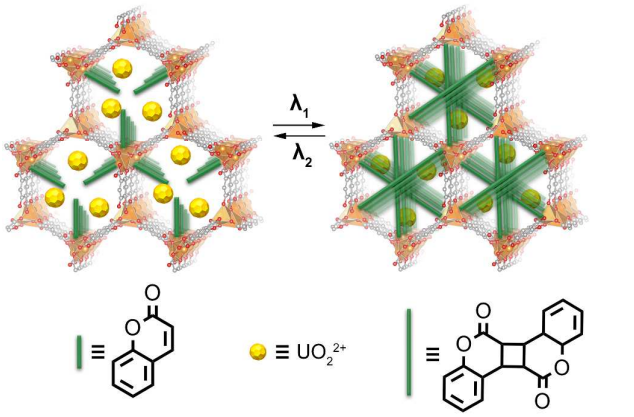

Fig. 16. Utilization of a MOF scaffold for the trapping and release of uranyl ions (yellow spheres) as a function of external stimuli. On demand release is achieved through photodimerization of coumarin upon irradiation with a different wavelength of light (short green post = coumarin molecules, long green post = coumarin dimer). Orange, grey, and red spheres represent zinc, carbon, and oxygen atoms of the framework, respectively.

harvesting, energy transfer, and photocatalysis are facets, which could be implemented towards the rational construction of a novel platform with unrevealed sensing benefits. The natural photosystem could be utilized as a model for integration of the mentioned photophysical processes inside a single MOF-based material creating a "three-in-one" sensing platform.

MOFs offer a great level of control for chromophore arrangements and structural parameters, including distances, angles, molecular conformations through rational design of organic linkers and tunability of synthetic conditions. Since light harvesting is the first step for the development of novel MOF-based sensors of this kind, it is essential for these scaffolds to possess wide absorption profiles achieved through efficient coupling of multiple chromophores.

Among the discussed directions, ET in MOFs has already been successfully applied towards efficient sensing of metal cations, explosives, organic solvents, and selected anions. Furthermore, MOF sensors coupled to ET have also found their applications for development of non-invasive thermometers. In addition to tunability and high surface area, the main advantage to develop ET-based sensors using a MOF is framework crystallinity, which allows for the precise determination of the distances and angles between self-assembled organic linkers, and therefore, modeling of short- and long-range ET processes.

Out of the three aspects of the natural photosystem that MOFs can replicate, one of the most intriguing is the phenomenon focused on the mimic of the photosystem reaction center since MOFs have already established themselves as efficient heterogeneous catalysts. The question still remains, however, of how to use photocatalysis in MOFs as a pathway for subsequent sensing. One of the possible approaches, which could be implemented through photocatalysis, is formation of analytes, which their predecessors are not feasible to detect (i.e., before their chemical transformations).

Another research area, which MOFs have the potential to impact for sensing advancement, is the engineering of photoresponsive sensors through integration of photochromic compounds inside a MOF matrix. Photochromic sensors possess a number of advantages such as multiple signal outputs leading to more information for analysis or recognition tuned as a function of photoisomerization. Furthermore, MOFs can be viewed as the next generation of "smart materials," whose sensing ability is controlled as a function of the external stimuli, including excitation wavelength, heat, pressure, or pH.

Due to porosity and structural modularity, MOFs can also be employed as tunable nanoreactors, with the potential to act as a "sensor-flask," i.e., promoting photocatalysis with subsequent size exclusion sensing.

To summarize, MOFs have the boundless potential to add a new disposition to the utilization of the "triple nature" of MOFs to boost sensor development. While a true three-in-one platform is yet to be realized, examples of two-in-one systems that highlight the interplay between light harvesting/ET or ET/sensing have been developed,[71,82,133] which demonstrates the feasibility of the proposed approach. However, integration of all the discussed aspects inside one material, along with the integration into a sensing device, is still an inexhaustible challenge.

Conflicts of interest

There are no conflicts to declare.

Acknowledgements

N.B.S. gratefully acknowledges support from the NSF CAREER Award (DMR-1553634) and a Cottrell Scholar Award from the Research Corporation for Science Advancement. N.B.S. also acknowledges the support from the Sloan Research Fellowship provided by Alfred P. Sloan Foundation.

References:

1 L. E. Kreno, K. Leong, O. K. Farha, M. Allendorf, R. P. Van Duyne and J. T. Hupp, *Chem. Rev.*, 2012, **112**, 1105–1125.
2 X. Zhang, W. Wang, Z. Hu, G. Wang and K. Uvdal, *Coord. Chem. Rev.*, 2015, **284**, 206–235.
3 Z. Hu, B. J. Deibert and J. Li, *Chem Soc Rev*, 2014, **43**, 5815–5840.
4 V. Stavila, A. A. Talin and M. D. Allendorf, *Chem. Soc. Rev.*, 2014, **43**, 5994–6010.
5 Y. Cui, Y. Yue, G. Qian and B. Chen, *Chem. Rev.*, 2012, **112**, 1126–1162.
6 J. Heine and K. Müller-Buschbaum, *Chem. Soc. Rev.*, 2013, **42**, 9232–9242.
7 K. Müller-Buschbaum, F. Beuerle and C. Feldmann, *Microporous Mesoporous Mater.*, 2015, **216**, 171–199.
8 L. Zhang, Z. Kang, X. Xin and D. Sun, *CrystEngComm*, 2016, **18**, 193–206.
9 F.-Y. Yi, D. Chen, M.-K. Wu, L. Han and H.-L. Jiang, *Chempluschem*, 2016, **81**, 675–690.
10 H. Xu, C.-S. Cao, X.-M. Kang and B. Zhao, *Dalt. Trans.*, 2016, **45**, 18003–18017.
11 Y. Zhang, S. Yuan, G. Day, X. Wang, X. Yang and H.-C. Zhou, *Coord. Chem. Rev.*, 2018, **354**, 28–45.
12 P. Mahata, S. K. Mondal, D. K. Singha and P. Majee, *Dalt. Trans.*, 2017, **46**, 301–328.
13 W. P. Lustig, S. Mukherjee, N. D. Rudd, A. V. Desai, J. Li and S. K. Ghosh, *Chem. Soc. Rev.*, 2017, **46**, 3242–3285.
14 M. D. Allendorf, C. A. Bauer, R. K. Bhakta and R. J. T. Houk, *Chem. Soc. Rev.*, 2009, **38**, 1330–1352.
15 L. Heinke, M. Tu, S. Wannapaiboon, R. A. Fischer and C. Wöll, *Microporous Mesoporous Mater.*, 2015, **216**, 200–215.
16 R. Medishetty, J. K. Zaręba, D. Mayer, M. Samoć and R. A. Fischer, *Chem. Soc. Rev.*, 2017, **46**, 4976–5004.
17 P. Silva, S. M. F. Vilela, J. P. C. Tomé and F. A. Almeida Paz, *Chem. Soc. Rev.*, 2015, **44**, 6774–6803.
18 D. Liu, K. Lu, C. Poon and W. Lin, *Inorg. Chem.*, 2014, **53**, 1916–1924.
19 Y. Cui, B. Li, H. He, W. Zhou, B. Chen and G. Qian, *Acc. Chem. Res.*, 2016, **49**, 483–493.
20 M.-H. Sun, S.-Z. Huang, L.-H. Chen, Y. Li, X.-Y. Yang, Z.-Y. Yuan and B.-L. Su, *Chem. Soc. Rev.*, 2016, **45**, 3479–3563.
21 J. Hao, X. Xu, H. Fei, L. Li and B. Yan, *Adv. Mater.*, 2018, 1705634.
22 B. Li, H.-M. Wen, Y. Cui, W. Zhou, G. Qian and B. Chen, *Adv. Mater.*, 2016, **28**, 8819–8860.

23 A. Bétard and R. A. Fischer, *Chem. Rev.*, 2012, **112**, 1055–1083.
24 O. Shekhah, J. Liu, R. A. Fischer and C. Wöll, *Chem. Soc. Rev.*, 2011, **40**, 1081–1106.
25 D. Bradshaw, A. Garai and J. Huo, *Chem. Soc. Rev.*, 2012, **41**, 2344–2381.
26 M. K. Smith and K. A. Mirica, *J. Am. Chem. Soc.*, 2017, **139**, 16759–16767.
27 E. A. Dolgopolova, O. A. Ejegbavwo, C. R. Martin, M. D. Smith, W. Setyawan, S. G. Karakalos, C. H. Henager, H.-C. zur Loye and N. B. Shustova, *J. Am. Chem. Soc.*, 2017, **139**, 16852–16861.
28 E. A. Dolgopolova, A. J. Brandt, O. A. Ejegbavwo, A. S. Duke, T. D. Maddumapatabandi, R. P. Galhenage, B. W. Larson, O. G. Reid, S. C. Ammal, A. Heyden, M. Chandrashekhar, V. Stavila, D. A. Chen and N. B. Shustova, *J. Am. Chem. Soc.*, 2017, **139**, 5201–5209.
29 S. Dang, X. Min, W. Yang, F. Y. Yi, H. You and Z. M. Sun, *Chem. - A Eur. J.*, 2013, **19**, 17172–17179.
30 J.-M. Zhou, W. Shi, H. H.-M. Li, H. H.-M. Li and P. Cheng, *J. Phys. Chem. C*, 2014, **118**, 416–426.
31 T. Lee, M. H. Tsai and H. L. Lee, *Cryst. Growth Des.*, 2012, **12**, 3181–3190.
32 H. Xu, Z. Dou, Y. Cui, B. Chen and G. Qian, *Chem. Commun.*, 2011, **47**, 3153–3155.
33 H. Tan, B. Liu and Y. Chen, *ACS Nano*, 2012, **6**, 10505–10511.
34 J.-M. Zhou, W. Shi, H. H.-M. Li, H. H.-M. Li and P. Cheng, *J. Phys. Chem. C*, 2014, **118**, 416–426.
35 J. M. Zhou, W. Shi, N. Xu and P. Cheng, *Inorg. Chem.*, 2013, **52**, 8082–8090.
36 Y. Cui, F. Zhu, B. Chen and G. Qian, *Chem. Commun.*, 2015, **51**, 7420–7431.
37 Y. Cui, H. Xu, Y. Yue, Z. Guo, J. Yu, Z. Chen, J. Gao, Y. Yang, G. Qian and B. Chen, *J. Am. Chem. Soc.*, 2012, **134**, 3979–3982.
38 Y. Cui, R. Song, J. Yu, M. Liu, Z. Wang, C. Wu, Y. Yang, Z. Wang, B. Chen and G. Qian, *Adv. Mater.*, 2015, **27**, 1420–1425.
39 A. Cadiau, C. D. S. Brites, P. M. F. J. Costa, R. A. S. Ferreira, J. Rocha and L. D. Carlos, *ACS Nano*, 2013, **7**, 7213–7218.
40 X. Liu, S. Akerboom, M. de Jong, I. Mutikainen, S. Tanase, A. Meijerink and E. Bouwman, *Inorg. Chem.*, 2015, **54**, 11323–11329.
41 X. Lian, D. Zhao, Y. Cui, Y. Yang and G. Qian, *Chem. Commun.*, 2015, **51**, 17676–17679.
42 J. Rocha, L. D. Carlos, F. A. A. Paz and D. Ananias, *Chem. Soc. Rev.*, 2011, **40**, 926–940.
43 C. Pagis, M. Ferbinteanu, G. Rothenberg and S. Tanase, *ACS Catal.*, 2016, **6**, 6063–6072.
44 A. Helal, Z. H. Yamani, K. E. Cordova and O. M. Yaghi, *Natl. Sci. Rev.*, 2017, **4**, 296–298.
45 S. M. Cohen, *J. Am. Chem. Soc.*, 2017, **139**, 2855–2863.
46 C. H. Hendon, A. J. Rieth, M. D. Korzyński and M. Dincă, *ACS Cent. Sci.*, 2017, **3**, 554–563.
47 W. Liu, K. Zhu, S. J. Teat, G. Dey, Z. Shen, L. Wang, D. M. O'Carroll and J. Li, *J. Am. Chem. Soc.*, 2017, **139**, 9281–9290.
48 J. Zhang, L. Wojtas, R. W. Larsen, M. Eddaoudi and M. J. Zaworotko, *J. Am. Chem. Soc.*, 2009, **131**, 17040–17041.
49 Z. Guo, D. K. Panda, M. A. Gordillo, A. Khatun, H. Wu, W. Zhou and S. Saha, *ACS Appl. Mater. Interfaces*, 2017, **9**, 32413–32417.
50 Q. Sun, B. Aguila, J. Perman, N. Nguyen and S. Ma, *J. Am. Chem. Soc.*, 2016, **138**, 15790–15796.
51 C. R. Murdock and D. M. Jenkins, *J. Am. Chem. Soc.*, 2014, **136**, 10983–10988.
52 C. R. Murdock, B. C. Hughes, Z. Lu and D. M. Jenkins, *Coord. Chem. Rev.*, 2014, **258–259**, 119–136.
53 S. Yuan, L. Zou, J.-S. Qin, J. Li, L. Huang, L. Feng, X. Wang, M. Bosch, A. Alsalme, T. Cagin and H.-C. Zhou, *Nat. Commun.*, 2017, **8**, 15356.
54 Q.-G. Zhai, X. Bu, X. Zhao, D.-S. Li and P. Feng, *Acc. Chem. Res.*, 2017, **50**, 407–417.
55 N. Baroni, A. Turshatov, M. Oldenburg, D. Busko, M. Adams, R. Haldar, A. Welle, E. Redel, C. Wöll, B. S. Richards and I. A. Howard, *Mater. Chem. Front.*, 2017, **1**, 1888–1894.
56 A. J. Howarth, A. W. Peters, N. A. Vermeulen, T. C. Wang, J. T. Hupp and O. K. Farha, *Chem. Mater.*, 2017, **29**, 26–39.
57 W. Lu, Z. Wei, Z.-Y. Gu, T.-F. Liu, J. Park, J. Park, J. Tian, M. Zhang, Q. Zhang, T. Gentle III, M. Bosch and H.-C. Zhou, *Chem. Soc. Rev.*, 2014, **43**, 5561–5593.
58 K. Sumida, K. Liang, J. Reboul, I. A. Ibarra, S. Furukawa and P. Falcaro, *Chem. Mater.*, 2017, **29**, 2626–2645.
59 D. Maspoch, D. Ruiz-Molina and J. Veciana, *Chem. Soc. Rev.*, 2007, **36**, 770–818.
60 N. C. Burtch, H. Jasuja and K. S. Walton, *Chem. Rev.*, 2014, **114**, 10575–10612.
61 H.-J. Son, S. Jin, S. Patwardhan, S. J. Wezenberg, N. C. Jeong, M. So, C. E. Wilmer, A. A. Sarjeant, G. C. Schatz, R. Q. Snurr, O. K. Farha, G. P. Wiederrecht and J. T. Hupp, *J. Am. Chem. Soc.*, 2013, **135**, 862–869.
62 J.-L. Wang, C. Wang and W. Lin, *ACS Catal.*, 2012, **2**, 2630–2640.
63 D. E. Williams and N. B. Shustova, *Chem. - A Eur. J.*, 2015, **21**, 15474–15479.
64 R. W. Larsen and L. Wojtas, *Dalt. Trans.*, 2015, **44**, 2959–2963.
65 T. Zhang and W. Lin, *Chem. Soc. Rev.*, 2014, **43**, 5982–5993.
66 M. C. So, G. P. Wiederrecht, J. E. Mondloch, J. T. Hupp and O. K. Farha, *Chem. Commun.*, 2015, **51**, 3501–3510.
67 E. A. Dolgopolova and N. B. Shustova, *MRS Bull.*, 2016, **41**, 890–896.
68 J. Liu, W. Zhou, J. Liu, I. Howard, G. Kilibarda, S. Schlabach, D. Coupry, M. Addicoat, S. Yoneda, Y. Tsutsui, T. Sakurai, S. Seki, Z. Wang, P. Lindemann, E. Redel, T. Heine and C. Wöll, *Angew. Chem. Int. Ed.*, 2015, **54**, 7441–7445.
69 X. Zhang, M. A. Ballem, Z.-J. Hu, P. Bergman and K. Uvdal, *Angew. Chem. Int. Ed.*, 2011, **50**, 5729–5733.
70 H. Yeo, K. Tanaka and Y. Chujo, *RSC Adv.*, 2017, **7**, 10869–10874.
71 C. Y. Lee, O. K. Farha, B. J. Hong, A. A. Sarjeant, S. T. Nguyen and J. T. Hupp, *J. Am. Chem. Soc.*, 2011, **133**, 15858–15861.
72 J. Zhu, W. A. Maza and A. J. Morris, *J. Photochem. Photobiol. A Chem.*, 2017, **344**, 64–77.
73 D. K. Panda, F. S. Goodson, S. Ray and S. Saha, *Chem. Commun.*, 2014, **50**, 5358–5360.
74 J. Aguilera-Sigalat and D. Bradshaw, *Coord. Chem. Rev.*, 2016, **307**, 267–291.
75 S.-N. Zhao, L.-J. Li, X.-Z. Song, M. Zhu, Z.-M. Hao, X. Meng, L.-L. Wu, J. Feng, S.-Y. Song, C. Wang and H.-J. Zhang, *Adv. Funct. Mater.*, 2015, **25**, 1463–1469.
76 M. A. Nasalevich, M. van der Veen, F. Kapteijn and J. Gascon, *CrystEngComm*, 2014, **16**, 4919–4926.
77 Y. Li, H. Xu, S. Ouyang and J. Ye, *Phys. Chem. Chem. Phys.*, 2016, **18**, 7563–7572.
78 L. Zeng, X. Guo, C. He and C. Duan, *ACS Catal.*, 2016, **6**, 7935–7947.
79 H. He, J. A. Perman, G. Zhu and S. Ma, *Small*, 2016, **12**, 6309–6324.
80 A. Dhakshinamoorthy, A. M. Asiri and H. García, *Angew. Chem. Int. Ed.*, 2016, **55**, 5414–5445.
81 S. Wang and X. Wang, *Small*, 2015, **11**, 3097–3112.
82 S. Jin, H.-J. Son, O. K. Farha, G. P. Wiederrecht and J. T. Hupp, *J. Am. Chem. Soc.*, 2013, **135**, 955–958.
83 R. Kaur, A. Rana, R. K. Singh, V. A. Chhabra, K.-H. Kim and A. Deep, *RSC Adv.*, 2017, **7**, 29015–29024.
84 L. Sun, H. Xing, Z. Liang, J. Yu and R. Xu, *Chem. Commun.*, 2013, **49**, 11155–11157.

85 K. Leong, M. E. Foster, B. M. Wong, E. D. Spoerke, D. Van Gough, J. C. Deaton and M. D. Allendorf, *J. Mater. Chem. A*, 2014, **2**, 3389–3398.
86 L. M. Lifshits, M. Zeller, C. F. Campana and J. K. Klosterman, *Cryst. Growth Des.*, 2017, **17**, 5449–5457.
87 L. M. Lifshits, B. C. Noll and J. K. Klosterman, *Chem. Commun.*, 2015, **51**, 11603–11606.
88 L. Ma, X. Feng, S. Wang and B. Wang, *Mater. Chem. Front.*, 2017, **1**, 2474–2486.
89 J. Mei, N. L. C. Leung, R. T. K. Kwok, J. W. Y. Lam and B. Z. Tang, *Chem. Rev.*, 2015, **115**, 11718–11940.
90 Y. Hong, J. W. Y. Lam and B. Z. Tang, *Chem. Soc. Rev.*, 2011, **40**, 5361–5388.
91 Z. Wei, Z.-Y. Gu, R. K. Arvapally, Y.-P. Chen, R. N. McDougald, J. F. Ivy, A. A. Yakovenko, D. Feng, M. A. Omary and H.-C. Zhou, *J. Am. Chem. Soc.*, 2014, **136**, 8269–8276.
92 N. B. Shustova, B. D. McCarthy and M. Dincă, *J. Am. Chem. Soc.*, 2011, **133**, 20126–20129.
93 N. B. Shustova, A. F. Cozzolino, S. Reineke, M. Baldo and M. Dincă, *J. Am. Chem. Soc.*, 2013, **135**, 13326–13329.
94 G. Lu and J. T. Hupp, *J. Am. Chem. Soc.*, 2010, **132**, 7832–7833.
95 J. R. Lakowicz, *Principles of Fluorescence Spectroscopy Principles of Fluorescence Spectroscopy*, 2006.
96 B. Valeur, *Molecular Fluorescence, Principles and Applications*, 2002.
97 Q. Zhang, C. Zhang, L. Cao, Z. Wang, B. An, Z. Lin, R. Huang, Z. Zhang, C. Wang and W. Lin, *J. Am. Chem. Soc.*, 2016, **138**, 5308–5315.
98 D. E. Williams, J. A. Rietman, J. M. Maier, R. Tan, A. B. Greytak, M. D. Smith, J. A. Krause and N. B. Shustova, *J. Am. Chem. Soc.*, 2014, **136**, 11886–11889.
99 D. E. Williams, E. A. Dolgopolova, D. C. Godfrey, E. D. Ermolaeva, P. J. Pellechia, A. B. Greytak, M. D. Smith, S. M. Avdoshenko, A. A. Popov and N. B. Shustova, *Angew. Chem. Int. Ed.*, 2016, **55**, 9070–9074.
100 A. M. Rice, W. B. Fellows, E. A. Dolgopolova, A. B. Greytak, A. K. Vannucci, M. D. Smith, S. G. Karakalos, J. A. Krause, S. M. Avdoshenko, A. A. Popov and N. B. Shustova, *Angew. Chem. Int. Ed.*, 2017, **56**, 4525–4529.
101 W. B. Fellows, A. M. Rice, D. E. Williams, E. A. Dolgopolova, A. K. Vannucci, P. J. Pellechia, M. D. Smith, J. A. Krause and N. B. Shustova, *Angew. Chem. Int. Ed.*, 2016, **55**, 2195–2199.
102 J. A. J. Arpino, H. Czapinska, A. Piasecka, W. R. Edwards, P. Barker, M. J. Gajda, M. Bochtler and D. D. Jones, *J. Am. Chem. Soc.*, 2012, **134**, 13632–13640.
103 E. A. Dolgopolova, D. E. Williams, A. B. Greytak, A. M. Rice, M. D. Smith, J. A. Krause and N. B. Shustova, *Angew. Chem. Int. Ed.*, 2015, **54**, 13639–13643.
104 D. E. Williams, E. A. Dolgopolova, P. J. Pellechia, A. Palukoshka, T. J. Wilson, R. Tan, J. M. Maier, A. B. Greytak, M. D. Smith, J. A. Krause and N. B. Shustova, *J. Am. Chem. Soc.*, 2015, **137**, 2223–2226.
105 M. T. Dang, L. Hirsch and G. Wantz, *Adv. Mater.*, 2011, **23**, 3597–3602.
106 D. Chen, A. Nakahara, D. Wei, D. Nordlund and T. P. Russell, *Nano Lett.*, 2011, **11**, 561–567.
107 A. M. Rice, E. A. Dolgopolova and N. B. Shustova, *Chem. Mater.*, 2017, **29**, 7054–7061.
108 J. Sukegawa, C. Schubert, X. Zhu, H. Tsuji, D. M. Guldi and E. Nakamura, *Nat. Chem.*, 2014, **6**, 899–905.
109 C.-Z. Li, H.-L. Yip and A. K.-Y. Jen, *J. Mater. Chem.*, 2012, **22**, 4161–4177.
110 F. Diederich and M. Gómez-López, *Chem. Soc. Rev.*, 1999, **28**, 263–277.
111 A. M. Butterfield, B. Gilomen and J. S. Siegel, *Org. Process Res. Dev.*, 2012, **16**, 664–676.
112 L. Zoppi, L. Martin-Samos and K. K. Baldridge, *Phys. Chem. Chem. Phys.*, 2015, **17**, 6114–6121.
113 L. M. Roch, L. Zoppi, J. S. Siegel and K. K. Baldridge, *J. Phys. Chem. C*, 2017, **121**, 1220–1234.
114 L. Zoppi, L. Martin-Samos and K. K. Baldridge, *J. Am. Chem. Soc.*, 2011, **133**, 14002–14009.
115 L. Cao, Z. Lin, W. Shi, Z. Wang, C. Zhang, X. Hu, C. Wang and W. Lin, *J. Am. Chem. Soc.*, 2017, **139**, 7020–7029.
116 K. C. Park, C. Seo, G. Gupta, J. Kim and C. Y. Lee, *ACS Appl. Mater. Interfaces*, 2017, **9**, 38670–38677.
117 C. A. Kent, B. P. Mehl, L. Ma, J. M. Papanikolas, T. J. Meyer and W. Lin, *J. Am. Chem. Soc.*, 2010, **132**, 12767–12769.
118 C. A. Kent, D. Liu, A. Ito, T. Zhang, M. K. Brennaman, T. J. Meyer and W. Lin, *J. Mater. Chem. A*, 2013, **1**, 14982–14989.
119 C. A. Kent, D. Liu, T. J. Meyer and W. Lin, *J. Am. Chem. Soc.*, 2012, **134**, 3991–3994.
120 Z. Wang, Y. Liu, Z. Wang, L. Cao, Y. Zhao, C. Wang and W. Lin, *Chem. Commun.*, 2017, **53**, 9356–9359.
121 J. An, C. M. Shade, D. A. Chengelis-Czegan, S. Petoud and N. L. Rosi, *J. Am. Chem. Soc.*, 2011, **133**, 1220–1223.
122 Y. Zheng, K. Liu, X. Sun, R. Guan, H. Su, H. You and C. Qi, *CrystEngComm*, 2015, **17**, 2321–2326.
123 E. Feijó de Melo, N. da C. Santana, K. G. Bezerra Alves, G. F. de Sá, C. Pinto de Melo, M. O. Rodrigues and S. A. Júnior, *J. Mater. Chem. C*, 2013, **1**, 7574–7581.
124 X.-Y. Li, W.-J. Shi, X.-Q. Wang, L.-N. Ma, L. Hou and Y.-Y. Wang, *Cryst. Growth Des.*, 2017, **17**, 4217–4224.
125 W. A. Maza, R. Padilla and A. J. Morris, *J. Am. Chem. Soc.*, 2015, **137**, 8161–8168.
126 X. Rao, T. Song, J. Gao, Y. Cui, Y. Yang, C. Wu, B. Chen and G. Qian, *J. Am. Chem. Soc.*, 2013, **135**, 15559–15564.
127 P. R. Matthes, C. J. Höller, M. Mai, J. Heck, S. J. Sedlmaier, S. Schmiechen, C. Feldmann, W. Schnick and K. Müller-Buschbaum, *J. Mater. Chem.*, 2012, **22**, 10179–10187.
128 E. A. Dolgopolova, T. M. Moore, W. B. Fellows, M. D. Smith and N. B. Shustova, *Dalt. Trans.*, 2016, **45**, 9884–9891.
129 E. A. Dolgopolova, A. M. Rice, M. D. Smith and N. B. Shustova, *Inorg. Chem.*, 2016, **55**, 7257–7264.
130 E. A. Dolgopolova, T. M. Moore, O. A. Ejegbavwo, P. J. Pellechia, M. D. Smith and N. B. Shustova, *Chem. Commun.*, 2017, **53**, 7361–7364.
131 D. Yan, Y. Tang, H. Lin and D. Wang, *Sci. Rep.*, 2015, **4**, 4337.
132 L.-H. Cao, H.-Y. Li, H. Xu, Y.-L. Wei and S.-Q. Zang, *Dalt. Trans.*, 2017, **46**, 11656–11663.
133 Y. Du, X. Li, X. Lv and Q. Jia, *ACS Appl. Mater. Interfaces*, 2017, **9**, 30925–30932.
134 N. Corrigan, S. Shanmugam, J. Xu and C. Boyer, *Chem. Soc. Rev.*, 2016, **45**, 6165–6212.
135 J. M. R. Narayanam and C. R. J. Stephenson, *Chem. Soc. Rev.*, 2011, **40**, 102–113.
136 D. Ravelli, M. Fagnoni and A. Albini, *Chem. Soc. Rev. Chem. Soc. Rev*, 2013, **42**, 97–113.
137 X. Yu, L. Wang and S. M. Cohen, *CrystEngComm*, 2017, **19**, 4126–4136.
138 H. Assi, G. Mouchaham, N. Steunou, T. Devic and C. Serre, *Chem. Soc. Rev.*, 2017, **46**, 3431–3452.
139 A. L. Linsebigler, G. Lu and J. T. Yates, *Chem. Rev.*, 1995, **95**, 735–758.
140 Y. Ma, X. Wang, Y. Jia, X. Chen, H. Han and C. Li, *Chem. Rev.*, 2014, **114**, 9987–10043.
141 M. D. Hernández-Alonso, F. Fresno, S. Suárez and J. M. Coronado, *Energy Environ. Sci.*, 2009, **2**, 1231–1257.
142 J. Schneider, M. Matsuoka, M. Takeuchi, J. Zhang, Y. Horiuchi, M. Anpo and D. W. Bahnemann, *Chem. Rev.*, 2014, **114**, 9919–9986.
143 H. L. Nguyen, *New J. Chem.*, 2017, **41**, 14030–14043.

144 M. Dan-Hardi, C. Serre, T. Frot, L. Rozes, G. Maurin, C. Sanchez and G. Férey, *J. Am. Chem. Soc.*, 2009, **131**, 10857–10859.
145 C. H. Hendon, D. Tiana, M. Fontecave, C. Sanchez, L. D'arras, C. Sassoye, L. Rozes, C. Mellot-Draznieks and A. Walsh, *J. Am. Chem. Soc.*, 2013, **135**, 10942–10945.
146 Y. Fu, D. Sun, Y. Chen, R. Huang, Z. Ding, X. Fu and Z. Li, *Angew. Chemie Int. Ed.*, 2012, **51**, 3364–3367.
147 M. B. Chambers, X. Wang, L. Ellezam, O. Ersen, M. Fontecave, C. Sanchez, L. Rozes and C. Mellot-Draznieks, *J. Am. Chem. Soc.*, 2017, **139**, 8222–8228.
148 H. L. Nguyen, F. Gándara, H. Furukawa, T. L. H. Doan, K. E. Cordova and O. M. Yaghi, *J. Am. Chem. Soc.*, 2016, **138**, 4330–4333.
149 H. L. Nguyen, T. T. Vu, D. Le, T. L. H. Doan, V. Q. Nguyen and N. T. S. Phan, *ACS Catal.*, 2017, **7**, 338–342.
150 K. G. M. Laurier, F. Vermoortele, R. Ameloot, D. E. De Vos, J. Hofkens and M. B. J. Roeffaers, *J. Am. Chem. Soc.*, 2013, **135**, 14488–14491.
151 D. Wang, M. Wang and Z. Li, *ACS Catal.*, 2015, **5**, 6852–6857.
152 D. Wang and Z. Li, *Catal. Sci. Technol.*, 2015, **5**, 1623–1628.
153 M. A. Ischay, M. E. Anzovino, J. Du and T. P. Yoon, *J. Am. Chem. Soc.*, 2008, **130**, 12886–12887.
154 D. A. Nicewicz and D. W. C. MacMillan, *Science (80-.).*, 2008, **322**, 77–80.
155 A. G. Condie, J. C. González-Gómez and C. R. J. Stephenson, *J. Am. Chem. Soc.*, 2010, **132**, 1464–1465.
156 M. Rueping, C. Vila, A. Szadkowska, R. M. Koenigs and J. Fronert, *ACS Catal.*, 2012, **2**, 2810–2815.
157 Y.-Q. Zou, J.-R. Chen, X.-P. Liu, L.-Q. Lu, R. L. Davis, K. A. Jørgensen and W.-J. Xiao, *Angew. Chem. Int. Ed.*, 2012, **51**, 784–788.
158 J.-M. Zen, S.-L. Liou, A. S. Kumar and M.-S. Hsia, *Angew. Chem. Int. Ed.*, 2003, **42**, 577–579.
159 C. Wang, Z. Xie, K. E. DeKrafft and W. Lin, *J. Am. Chem. Soc.*, 2011, **133**, 13445–13454.
160 X. Yu and S. M. Cohen, *Chem. Commun.*, 2015, **51**, 9880–9883.
161 X. Yu and S. M. Cohen, *J. Am. Chem. Soc.*, 2016, **138**, 12320–12323.
162 K. M. Kadish, K. M. Smith and R. Guilard, *The Porphyrin Handbook*, 2012.
163 W.-Y. Gao, M. Chrzanowski and S. Ma, *Chem. Soc. Rev.*, 2014, **43**, 5841–5866.
164 S. Yuan, T.-F. Liu, D. Feng, J. Tian, K. Wang, J. Qin, Q. Zhang, Y.-P. Chen, M. Bosch, L. Zou, S. J. Teat, S. J. Dalgarno and H.-C. Zhou, *Chem. Sci.*, 2015, **6**, 3926–3930.
165 T. Dilbeck, J. C. Wang, Y. Zhou, A. Olsson, M. Sykora and K. Hanson, *J. Phys. Chem. C*, 2017, **121**, 19690–19698.
166 M. Kaushal, A. L. Ortiz, J. A. Kassel, N. Hall, T. D. Lee, G. Singh and M. G. Walter, *J. Mater. Chem. C*, 2016, **4**, 5602–5609.
167 D. Feng, Z.-Y. Gu, J.-R. Li, H.-L. Jiang, Z. Wei and H.-C. Zhou, *Angew. Chem. Int. Ed.*, 2012, **51**, 10307–10310.
168 D. Feng, W.-C. Chung, Z. Wei, Z.-Y. Gu, H.-L. Jiang, Y.-P. Chen, D. J. Darensbourg and H.-C. Zhou, *J. Am. Chem. Soc.*, 2013, **135**, 17105–17110.
169 X.-S. Wang, L. Meng, Q. Cheng, C. Kim, L. Wojtas, M. Chrzanowski, Y.-S. Chen, X. P. Zhang and S. Ma, *J. Am. Chem. Soc.*, 2011, **133**, 16322–16325.
170 L. Meng, Q. Cheng, C. Kim, W.-Y. Gao, L. Wojtas, Y.-S. Chen, M. J. Zaworotko, X. P. Zhang and S. Ma, *Angew. Chem. Int. Ed.*, 2012, **51**, 10082–10085.
171 Z. Zhang, L. Zhang, L. Wojtas, P. Nugent, M. Eddaoudi and M. J. Zaworotko, *J. Am. Chem. Soc.*, 2012, **134**, 924–927.
172 S. Takaishi, E. J. DeMarco, M. J. Pellin, O. K. Farha and J. T. Hupp, *Chem. Sci.*, 2013, **4**, 1509–1513.
173 J. A. Johnson, X. Zhang, T. C. Reeson, Y.-S. Chen and J. Zhang, *J. Am. Chem. Soc.*, 2014, **136**, 15881–15884.
174 J. A. Johnson, J. Luo, X. Zhang, Y.-S. Chen, M. D. Morton, E. Echeverría, F. E. Torres and J. Zhang, *ACS Catal.*, 2015, **5**, 5283–5291.
175 M.-H. Xie, X.-L. Yang, C. Zou and C.-D. Wu, *Inorg. Chem.*, 2011, **50**, 5318–5320.
176 D. W. C. MacMillan, *Nature*, 2008, **455**, 304–308.
177 N. A. Romero and D. A. Nicewicz, *Chem. Rev.*, 2016, **116**, 10075–10166.
178 L. Huang, J. Zhao, S. Guo, C. Zhang and J. Ma, *J. Org. Chem.*, 2013, **78**, 5627–5637.
179 G. N. Papadopoulos and C. G. Kokotos, *Chem. - A Eur. J.*, 2016, **22**, 6964–6967.
180 E. Arceo, E. Montroni and P. Melchiorre, *Angew. Chem. Int. Ed.*, 2014, **53**, 12064–12068.
181 Y. Liu, D. Chen, X. Li, Z. Yu, Q. Xia, D. Liang and H. Xing, *Green Chem.*, 2016, **18**, 1475–1481.
182 Q.-Y. Li, Z. Ma, W.-Q. Zhang, J.-L. Xu, W. Wei, H. Lu, X. Zhao and X.-J. Wang, *Chem. Commun.*, 2016, **52**, 11284–11287.
183 P. Wu, C. He, J. Wang, X. Peng, X. Li, Y. An and C. Duan, *J. Am. Chem. Soc.*, 2012, **134**, 14991–14999.
184 A. Atilgan, T. Islamoglu, A. J. Howarth, J. T. Hupp and O. K. Farha, *ACS Appl. Mater. Interfaces*, 2017, **9**, 24555–24560.
185 A. J. Howarth, C. T. Buru, Y. Liu, A. M. Ploskonka, K. J. Hartlieb, M. McEntee, J. J. Mahle, J. H. Buchanan, E. M. Durke, S. S. Al-Juaid, J. F. Stoddart, J. B. DeCoste, J. T. Hupp and O. K. Farha, *Chem. - A Eur. J.*, 2017, **23**, 214–218.
186 L. Zeng, T. Liu, C. He, D. Shi, F. Zhang and C. Duan, *J. Am. Chem. Soc.*, 2016, **138**, 3958–3961.
187 Y.-Z. Chen and H.-L. Jiang, *Chem. Mater.*, 2016, **28**, 6698–6704.
188 M. Lismont, L. Dreesen and S. Wuttke, *Adv. Funct. Mater.*, 2017, **27**, 1606314.
189 A. A. Beharry, *Biochemistry*, 2018, **57**, 173–174.
190 K. Lu, C. He and W. Lin, *J. Am. Chem. Soc.*, 2014, **136**, 16712–16715.
191 W. Wang, L. Wang, Z. Li and Z. Xie, *Chem. Commun.*, 2016, **52**, 5402–5405.
192 R. Pardo, M. Zayat and D. Levy, *Chem. Soc. Rev.*, 2011, **40**, 672–687.
193 C. D. Jones and J. W. Steed, *Chem. Soc. Rev.*, 2016, **45**, 6546–6596.
194 S. Kawata and Y. Kawata, *Chem Rev*, 2000, **100**, 1777–1788.
195 M. Irie, T. Fukaminato, K. Matsuda and S. Kobatake, *Chem. Rev.*, 2014, **114**, 12174–12277.
196 J. Zhang, Q. Zou and H. Tian, *Adv. Mater.*, 2013, **25**, 378–399.
197 M. Qin, Y. Huang, F. Li and Y. Song, *J. Mater. Chem. C*, 2015, **3**, 9265–9275.
198 G. Mehlana and S. A. Bourne, *CrystEngComm*, 2017, **19**, 4238–4259.
199 S. Castellanos, F. Kapteijn and J. Gascon, *CrystEngComm*, 2016, **18**, 4006–4012.
200 R. D. Mukhopadhyay, V. K. Praveen and A. Ajayaghosh, *Mater. Horiz.*, 2014, **1**, 572–576.
201 A. Schneemann, V. Bon, I. Schwedler, I. Senkovska, S. Kaskel and R. A. Fischer, *Chem. Soc. Rev.*, 2014, **43**, 6062–6096.
202 F.-X. Coudert, *Chem. Mater.*, 2015, **27**, 1905–1916.
203 M. Zhang, M. Bosch, T. Gentle III and H.-C. Zhou, *CrystEngComm*, 2014, **16**, 4069–4083.
204 B. Gui, Y. Meng, Y. Xie, K. Du, A. C. H. Sue and C. Wang, *Macromol. Rapid Commun.*, 2017, 1700388.
205 M.-M. Russew and S. Hecht, *Adv. Mater.*, 2010, **22**, 3348–3360.
206 R. Klajn, *Chem. Soc. Rev.*, 2014, **43**, 148–184.
207 Y. Zheng, H. Sato, P. Wu, H. J. Jeon, R. Matsuda and S. Kitagawa, *Nat. Commun.*, 2017, **8**, 100.

208 V. I. Nikolayenko, S. A. Herbert and L. J. Barbour, *Chem. Commun.*, 2017, **53**, 11142–11145.
209 L. Le Gong, W. T. Yao, Z. Q. Liu, A. M. Zheng, J. Q. Li, X. F. Feng, L. F. Ma, C. S. Yan, M. B. Luo and F. Luo, *J. Mater. Chem. A*, 2017, **5**, 7961–7967.
210 R. Lyndon, K. Konstas, B. P. Ladewig, P. D. Southon, P. C. J. Kepert and M. R. Hill, *Angew. Chem. Int. Ed.*, 2013, **52**, 3695–3698.
211 Shih-Sheng Sun, A. Jason A. Anspach and A. J. Lees, *Inorg. Chem.*, 2002, **41**, 1862–1869.
212 C. Bin Fan, Z. Q. Liu, L. Le Gong, A. M. Zheng, L. Zhang, C. S. Yan, H. Q. Wu, X. F. Feng and F. Luo, *Chem. Commun.*, 2017, **53**, 763–766.
213 A. B. Kanj, K. Müller and L. Heinke, *Macromol. Rapid Commun.*, 2017, 1700239.
214 J. Park, D. Yuan, K. T. Pham, J. R. Li, A. Yakovenko and H. C. Zhou, *J. Am. Chem. Soc.*, 2012, **134**, 99–102.
215 Z. Wang, L. Heinke, J. Jelic, M. Cakici, M. Dommaschk, R. J. Maurer, H. Oberhofer, S. Grosjean, R. Herges, S. Bräse, K. Reuter and C. Wöll, *Phys. Chem. Chem. Phys.*, 2015, **17**, 14582–14587.
216 X. Meng, B. Gui, D. Yuan, M. Zeller and C. Wang, *Sci. Adv.*, 2016, **2**, 1600480.
217 K. Healey, W. Liang, P. D. Southon, T. L. Church and D. M. D'Alessandro, *J. Mater. Chem. A*, 2016, **4**, 10816–10819.
218 D. G. Patel, I. M. Walton, J. M. Cox, C. J. Gleason, D. R. Butzer and J. B. Benedict, *Chem. Commun.*, 2014, **50**, 2653–2656.
219 I. M. Walton, J. M. Cox, C. A. Benson, D. G. Patel, Y.-S. Chen and J. B. Benedict, *New J. Chem.*, 2016, **40**, 101–106.
220 I. M. Walton, J. M. Cox, T. B. Mitchell, N. P. Bizier and J. B. Benedict, *CrystEngComm*, 2016, **18**, 7972–7977.
221 H. A. Schwartz, S. Olthof, D. Schaniel, K. Meerholz and U. Ruschewitz, *Inorg. Chem.*, 2017, **56**, 13100–13110.
222 N. Yanai, T. Uemura, M. Inoue, R. Matsuda, T. Fukushima, M. Tsujimoto, S. Isoda and S. Kitagawa, *J. Am. Chem. Soc.*, 2012, **134**, 4501–4504.
223 I. M. Walton, J. M. Cox, J. A. Coppin, C. M. Linderman, D. G. Patel and J. B. Benedict, *Chem. Commun.*, 2013, **49**, 8012–8014.
224 M. Otte, *ACS Catal.*, 2016, **6**, 6491–6510.
225 Y. Inokuma, M. Kawano and M. Fujita, *Nat. Chem.*, 2011, **3**, 349–358.
226 M. Yoshizawa, J. K. Klosterman and M. Fujita, *Angew. Chem. Int. Ed.*, 2009, **48**, 3418–3438.
227 T. Kawamichi, T. Kodama, M. Kawano and M. Fujita, *Angew. Chem. Int. Ed.*, 2008, **47**, 8030–8032.
228 W. J. Gee, *Dalt. Trans.*, 2017, **46**, 15979–15986.
229 S. R. Salpage, Y. Xu, B. Som, A. J. Sindt, M. D. Smith and L. S. Shimizu, *RSC Adv.*, 2016, **6**, 98350–98355.
230 M. Yoshizawa, Y. Takeyama, T. Kusukawa and M. Fujita, *Angew. Chemie Int. Ed.*, 2002, **41**, 1347–1349.
231 N. L. Rosi, J. Kim, M. Eddaoudi, B. Chen, M. O'Keeffe and O. M. Yaghi, *J. Am. Chem. Soc.*, 2005, **127**, 1504–1518.
232 L. Zhang, L. L. Wang, L. Le Gong, X. F. Feng, M. B. Luo and F. Luo, *J. Hazard. Mater.*, 2016, **311**, 30–36.
233 H. Sato, R. Matsuda, K. Sugimoto, M. Takata and S. Kitagawa, *Nat. Mater.*, 2010, **9**, 661–666.